Fig. 4

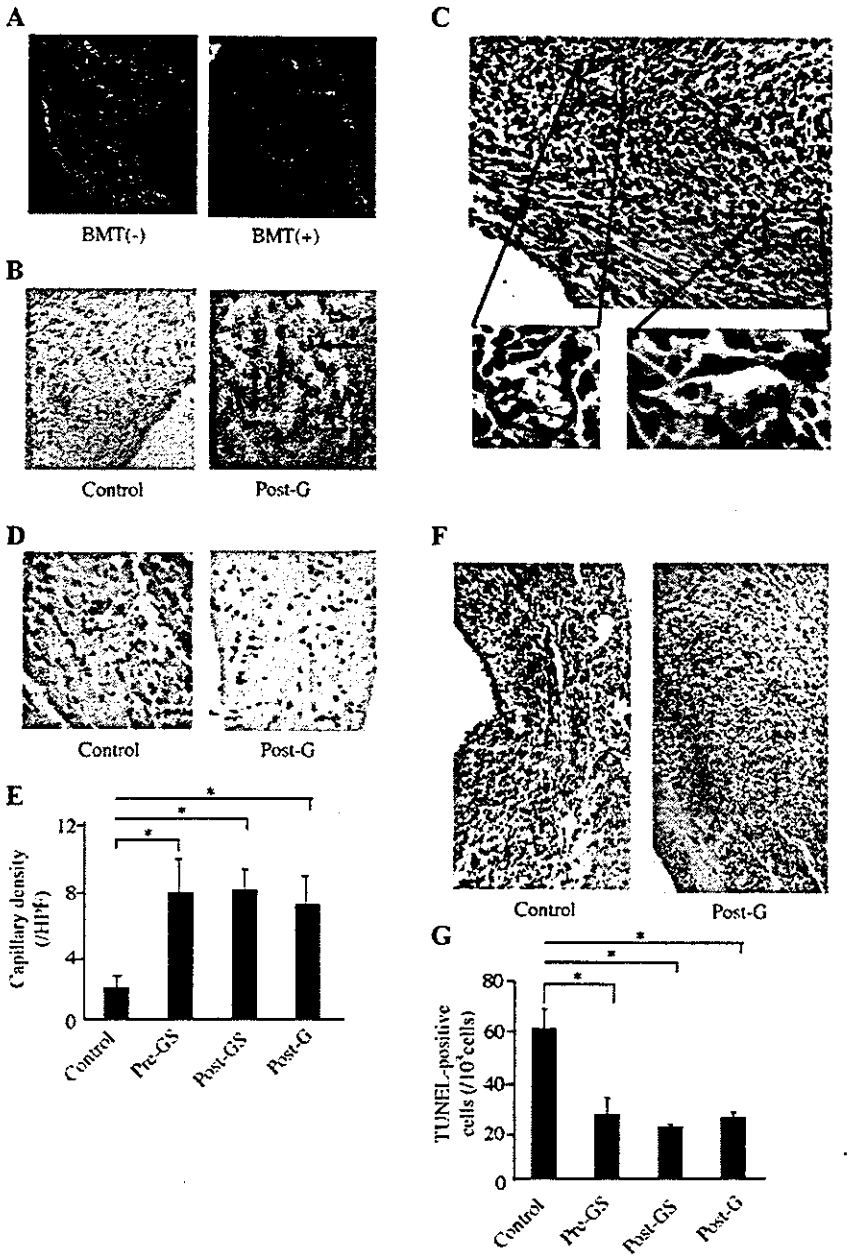

Figure 4. GFP-positive cells, capillary density and TUNEL-positive cells after MI. ***A***) Non-specific autofluorescence was recognized at the infarcted and border areas. BMT (–), infarcted heart of the mice without BM transplantation; BMT (+), infarcted heart of the mice whose BM was replaced with that of GFP mice. ***B***) Many GFP-positive cells (brown), which were mainly infiltrated blood cells, were recognized at the border area after MI in the three treatment groups with G-CSF. ***C***) GFP-positive cells were observed at capillary wall after MI in all the treatment groups. ***D***) The capillary density was examined by measuring PECAM-1-positive cells. ***E***) The density of capillaries at the border area was more increased in all the cytokine groups than in control group (*P<0.05). There was no significant difference of the capillary densities among the three treatment groups with G-CSF. ***F***) Apoptotic cells at Day 4 after MI. ***G***) The number of TUNEL-positive cells at the border area was less in all the treatment groups than in control group (*P<0.05). There was no significant difference in the number of TUNEL-positive cells among the three treatment groups.

Fig. 5

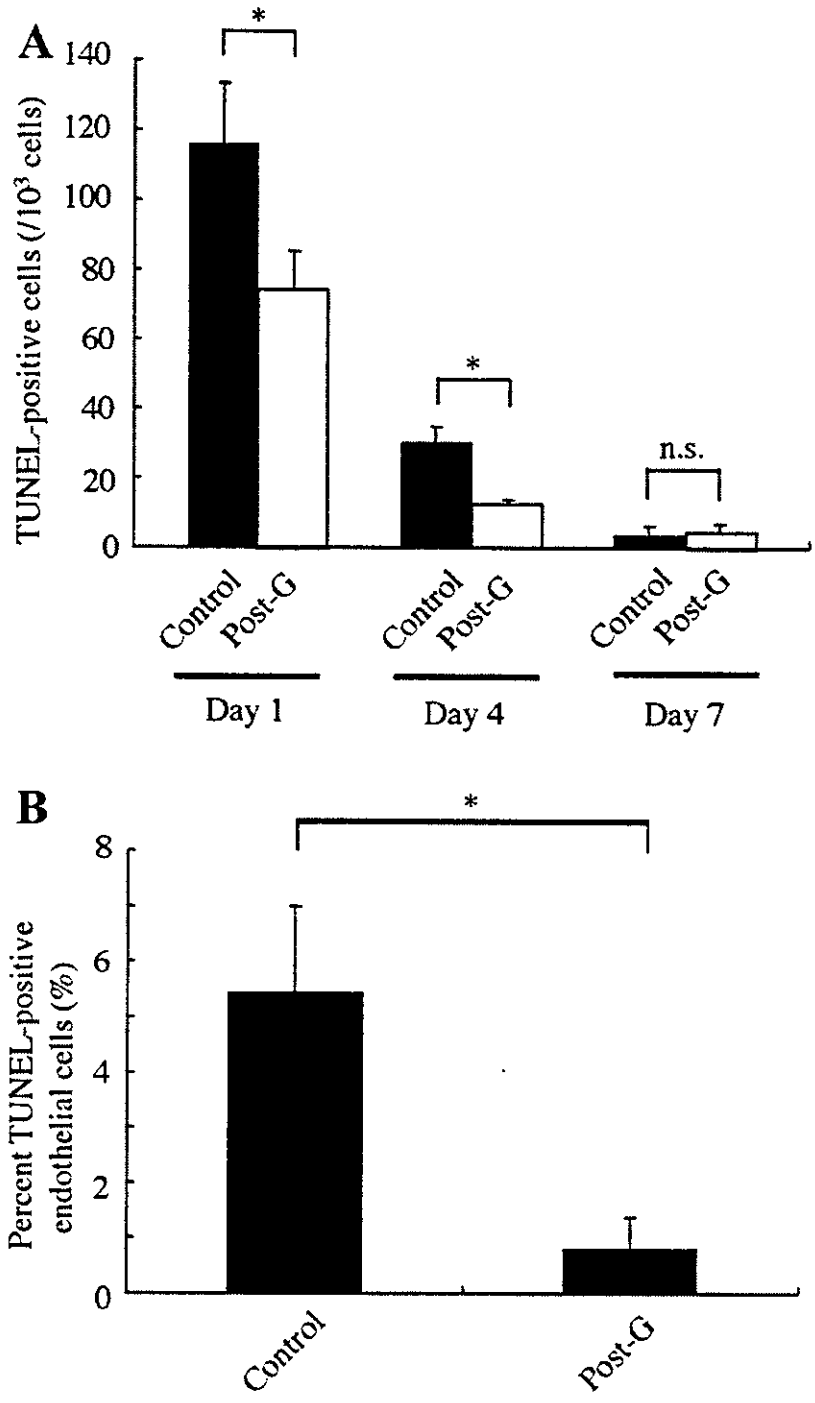

Figure 5. Apoptotic endothelial cell and non-endothelial cell death. *A)* At Day 1 and Day 4, the number of TUNEL-positive cells was significantly smallerin the Post-G group than in control group (*P<0.05). *B)* We checked double-immunohistochemical analysis to identify for the apoptotic endothelial cells at Day 1 after MI. The percentage of von Willebrand factor-positive cells in TUNEL-positive cells was significantly smaller in the Post-G group (*P<0.05).

Angiotensin II Type 1a Receptor Is Involved in Cell Infiltration, Cytokine Production, and Neovascularization in Infarcted Myocardium

Haruhiro Toko, Yunzeng Zou, Tohru Minamino, Masaya Sakamoto, Masanori Sano, Mutsuo Harada, Toshio Nagai, Takeshi Sugaya, Fumio Terasaki, Yasushi Kitaura, Issei Komuro

Objective—Angiotensin II is critically involved in left ventricular remodeling after myocardial infarction. Neovascularization has been thought to prevent the development of left ventricular remodeling and deterioration to heart failure. To elucidate the role of angiotensin II in neovascularization during cardiac remodeling, we induced myocardial infarction in angiotensin II type1a receptor (AT1) knockout (KO) mice.

Methods and Results—There were more vessels in the border zone of infarcted hearts of wild-type (WT) mice and AT1KO mice at 14 days after operation, compared with in the left ventricle of sham-operated mice, and the number was larger in WT mice than in AT1KO mice. Consistent with these observations, the infarcted heart of AT1KO mice expressed lower levels of matrix metalloproteinase and endothelial nitric oxide synthase activity. More inflammatory cells such as granulocytes and macrophages were infiltrated in the infarcted hearts of WT mice than AT1KO mice at 4 days. A variety of cytokines and chemokines were increased in infarcted hearts of WT and AT1KO mice, and many of them were more remarkable in WT mice than in AT1KO mice at 14 days.

Conclusions—AT1 plays a critical role in inflammatory cell infiltration, cytokine production, and neovascularization in infarcted hearts. (***Arterioscler Thromb Vasc Biol.* 2004;24:664-670.**)

Key Words: angiotensin II ■ AT1 receptor ■ neovascularization ■ myocardial infarction ■ cardiac remodeling

Left ventricular remodeling after myocardial infarction (MI) causes progression of heart failure and death. The remodeling process is characterized by progressive expansion of the initial infarct area and dilation of the left ventricular lumen, with cardiomyocyte replacement by fibrous tissue deposition in the ventricular wall. Once these processes develop, the infarcted heart accelerates the deterioration of ventricular dysfunction, leading to heart failure.

See page 622

Accumulating evidence has suggested that the renin-angiotensin system (RAS) plays an important role in left ventricular remodeling after MI, and that inhibition of RAS with angiotensin-converting enzyme (ACE) inhibitors and angiotensin II (AngII) type 1a receptor (AT1) blockers suppresses the cardiac remodeling and reduces the mortality after MI in clinical studies and experimental models.[1–3] We also reported that AngII plays a critical role in cardiac remodeling and mortality after MI using AT1 knockout (KO) mice.[4] Although cardiac dysfunction was more prominent and mortality was higher in wild-type (WT) mice than AT1KO mice after MI,[4] the precise mechanism of how AngII induces left ventricular remodeling remains unknown.

It has been reported that neovascularization within the infarcted tissue is an integral component of the remodeling process and that induction of neovascularization reduces infracted area and mortality.[5] There are several controversial reports regarding the effects of AngII on vascularization. Some reports have shown that AngII induces neovascularization in tumors, ischemic legs, and retina,[6–8] but others have reported that inhibition of RAS stimulates neovascularization.[9] It has also been reported that an ACE inhibitor does not inhibit vascular growth during the early phase of post-infarcted cardiac remodeling and scar formation.[10] To elucidate the role of AngII in neovascularization in the heart, we induced MI and examined the number of vessels in AT1KO mice.

Methods

Animals

Eight-week-old male WT mice and AT1KO mice[11] from the same genetic background were used in the present study (SLC, Shizuoka,

Received December 22, 2003; revision accepted January 21, 2004.

From the Department of Cardiovascular Science and Medicine (H.T., Y.Z., T.M., M. Sakamoto, M. Sano, M.H., T.N., I.K.), Chiba University Graduate School of Medicine, Chiba, Japan; Discovery Laboratory (T.S.), Tanabe Seiyaku Co, Ltd, Osaka, Japan; and Third Department of Internal Medicine (F.T., Y.K.), Osaka Medical College, Osaka, Japan.

Correspondence to Dr Issei Komuro, Department of Cardiovascular Science and Medicine, Chiba University Graduate School of Medicine, 1-8-1 Inohana, Chuo-ku, Chiba 260-8670, Japan. E-mail komuro-tky@umin.ac.jp

Arterioscler Thromb Vasc Biol. is available at http://www.atvbaha.org DOI: 10.1161/01.ATV.0000122361.63827.ab

Japan). Mice were housed under climate-controlled conditions with a 12-hour light/dark cycle and were provided with standard food and water ad libitum as described previously.[12] All protocols were approved by the Institutional Animal Care and Use Committee of Chiba University.

MI Model

MI was produced in male WT and AT1KO mice by left coronary artery ligation as described previously.[4] Mice were sacrificed at 1, 4, 7, and 14 days after the operation. Sham-operated control mice did not receive coronary artery ligation. Before procedure, systolic blood pressure (SBP) and heart rate were measured by using a tail-cuff method.[12]

Hydralazine Treatment

It has been reported that SBP was lower in AT1KO mice than WT mice.[11,13] To examine the effect of BP on angiogenesis, we administered hydralazine (Norvartis Pharmaceuticals, Tokyo, Japan) to WT mice. WT mice were treated with hydralazine (3 mg/kg per day) through osmotic mini pump (Alzet, Palo Alto, Calif)[14] from 1 week before procedure to euthanization. Our preliminary experiments showed that SBP in WT mice treated with this dose of hydralazine was similar to that in AT1KO mice.

Number of Capillaries and Arterioles

We examined neovascularization by measuring the number of capillaries and arterioles in light microscopic sections taken from the border zone of the infarcted heart. Capillary endothelial cells and smooth muscle α-actin (SMA) were identified by immunohistochemical staining with anti-platelet/endothelial cell adhesion molecule (PECAM) antibody and anti-SMA antibody (PROGEN Biotechnik GmbH, Heidelberg, Germany), respectively. Ten random microscopic fields were examined and the number of capillaries and arterioles were expressed as the number of PECAM-positive capillaries and SMA-positive arteriole/high-power field (HPF) (×400).[7]

Histological Analysis for Inflammatory Response

Immunohistochemical analysis was performed with anti-Ly6G antibody, anti-Mac3 antibody, and anti-CD3 antibody (BD Pharmingen, San Diego, Calif) to detect granulocytes, macrophages, and T lymphocytes, respectively, according to the supplier's instructions. We counted positive cells in 10 random microscopic HPFs.

Western Blot Analysis

Protein extracts were obtained after homogenization of infarcted myocardium: 100 μg of protein was separated on a polyacrylamide gel and electroblotted onto nitrocellulose transfer membrane (Schleicher & Schuell, Dassel, Germany). The membrane was blocked with 5% skim milk and 0.5% BSA in PBS with 0.1% Tween-20 (T-PBS) and then probed with anti-matrix metalloproteinase (MMP)-2 antibody, anti- MMP-9 antibody, anti-Akt antibody, anti-endothelial nitric oxide synthase (eNOS) antibody, and anti-phospho-Akt antibody (Cell Signaling, Beverly, Mass) for 1 hour at room temperature. After incubation with the primary antibody, the membrane was washed in T-PBS and was incubated for 1 hour with peroxidase-conjugated secondary antibody. The reaction was detected using ECL detection reagent kit (Amersham Pharmacia, Buckinghamshire, UK).

NOS Activity Assay and NOS Inhibition

The NOS activity (calcium-dependent) in infarcted myocardium was examined using NOS assay kit (Calbiochem, San Diego, Calif) according to the manufacture's instruction. To examine the role of eNOS in angiogenesis after MI, we administered a NOS inhibitor, N^G-nitro-L-arginine methyl ester (L-NAME) (4 mg/kg per day) via drinking water to WT mice from 1 week before procedure to euthanization.

Ribonuclease Protection Assay

Total RNA was extracted from left ventricles with RNAzol B (Biotecx Laboratories) and analyzed by ribonuclease protection assay. Multi-probes template sets, mCK-3b and mCK-5, were available with reagents of in vitro transcription and ribonuclease protection assay (RiboQuant; Pharmingen). For all hybridization assays, we used 2 μg total RNA from the sham-operated mice hearts and the MI hearts.

Implantation of Sarcoma Cells

S180 sarcoma was inoculated subcutaneously into the right axilla of male WT and AT1KO mice at a dose of 2×10^6 cells in 0.2 mL PBS/mouse.[15] The mice were euthanized on day 14, and the tumor was removed and weighted. The number of capillaries in the tumor was counted as described.

Statistical Analysis

Data were shown as mean±SEM. Multiple group comparison was performed by one-way ANOVA followed by the Bonferroni procedure for comparison of means. Comparison between 2 groups was analyzed by the two-tailed Student t test or two-way ANOVA. Values of $P<0.05$ were considered statistically significant.

Results

AT1 Plays a Critical Role in Neovascularization After MI

We have previously reported that an infarcted size was significantly reduced in AT1KO mice compared with WT mice.[4] We therefore examined whether AT1 was involved in angiogenesis during the remodeling process. Immunohistochemical studies using anti-PECAM antibody revealed that the number of capillaries was increased in the border zone of the infarcted hearts of WT and AT1KO mice 14 days after MI as compared with hearts of sham-operated mice (Figure 1A), and this increase was more prominent in WT mice than in AT1KO mice (Figure 1A and 1B). Immunohistochemical analysis using anti-SMA antibody showed that the number of arteriole was also increased in the border zone of the infarcted hearts of WT mice on day 14 after MI, but not of AT1KO mice (Figure 1C and 1D). These results suggest that AT1 has stimulating effects on neovascularization after MI.

There was no significant difference in the heart rate between WT mice and AT1KO mice, but SBP in AT1KO mice was lower than that in WT mice (Figure 1E), which might affect neovascularization. To examine the effect of BP on angiogenesis after MI, we administered hydralazine to WT mice. SBP in WT mice treated with hydralazine was as low as that in AT1KO mice (Figure 1E). There was no significant difference in the capillary density between WT mice with hydralazine and WT mice without the treatment (Figure 1F). These results indicate that lower BP of AT1KO did not account for decreased angiogenesis in ischemic myocardium.

AT1 Mediates Cell Infiltration After MI

Because it has been reported that inflammation is an important trigger for ischemia-induced neovascularization[16] and that the RAS plays an important role in inflammatory responses,[17] we examined infiltration of inflammatory cells in the heart after MI. The numbers of granulocytes, macrophages, and T lymphocytes were examined in the myocardium on day 4 after MI using anti-Ly6G, anti-Mac3, and anti-CD3 antibodies, respectively. Many granulocytes (Figure 2A and 2D), macrophages (Figure

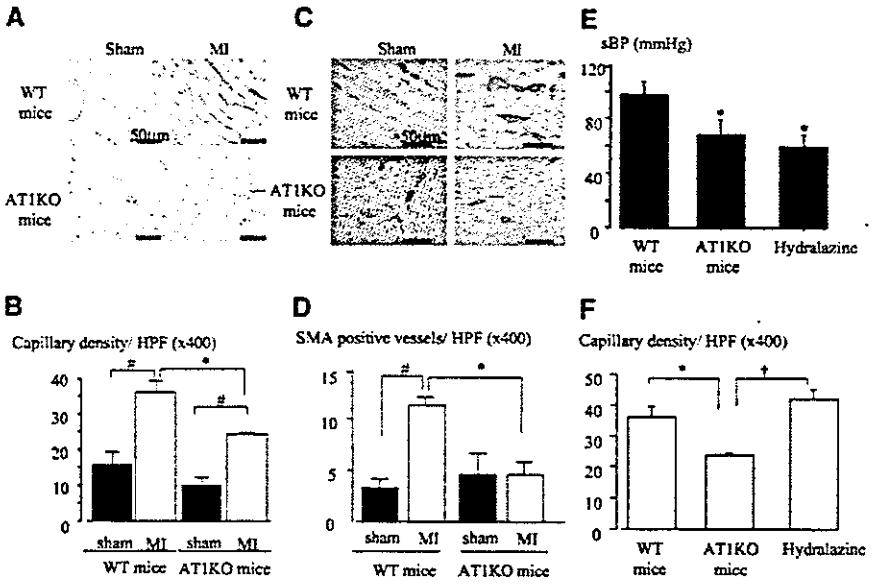

Figure 1. Neovascularization at 14 days after MI. A, The border zone of infarcted heart was stained with anti-PECAM antibody. B, Number of PECAM-positive capillaries per HPF. C, The border zone of infarcted heart was stained with anti-SMA antibody. D, Number of SMA-positive arterioles per HPF. E, Systolic blood pressure (SBP) before MI. F, Number of PECAM-positive capillaries per HPF. MI indicates myocardial infarction; WT, wild-type; AT1KO, angiotensin type1a receptor knockout; hydralazine, WT mice treated with hydralazine; HPF, high-power field. *$P<0.01$ versus WT, #$P<0.01$ versus sham, †$P<0.01$ versus AT1KO.

2B and 2E), and T lymphocytes (Figure 2C and 2F) were observed in the heart of WT and AT1KO mice after MI. The numbers of infiltrative cells such as granulocytes and macrophages were much larger in WT mice than those in AT1KO mice (Figure 2G), suggesting that AT1 is critically involved in cell infiltration in the myocardium after MI.

AT1 Induces MMPs and Activates Akt-1

Because it has been reported that MMPs are important for cell invasion into extravascular space[8] and that MMPs play a critical role in vascularization,[18] we next examined protein levels of MMP-2 and MMP-9 in the heart after MI. MMP-2 was increased on day 1 after MI in both WT mice and AT1KO mice (Figure 3A and 3B). MMP-9 was increased from day 4 in both WT mice and AT1KO mice (Figure 3A and 3C). The increases of MMP-2 and MMP-9 were more remarkable in WT mice compared with AT1KO mice (Figure 3B and 3C).

We examined another angiogenic factor, Akt-1.[19] The protein level of Akt-1 was increased in WT mice and AT1KO mice after MI (Figure 3D), and the increase was more prominent in WT mice (Figure 3E). The level of phosphorylated Akt-1 was more markedly increased after MI in WT mice than in AT1KO mice (Figure 3D and 3F), suggesting that AngII enhances activation of Akt-1 after MI.

Activation of eNOS by AngII Induces Angiogenesis

Akt has been shown to phosphorylate and activate eNOS,[20,21] thereby promoting angiogenesis.[22,23] We therefore examined the protein level and activity of NOS in the heart after MI. There was no significant change in eNOS protein levels after MI between WT mice and AT1KO mice (Figure 4A and 4B), but the NOS activity in WT mice was higher than that in AT1KO mice (Figure 4C). Expression of vascular endothelial growth factor after MI did not differ between WT mice and AT1KO mice (data not shown).

To further elucidate the role of eNOS activity in infarcted myocardium, we administered L-NAME to WT mice to reduce NO production. Treatment with L-NAME partially but significantly reduced the capillary density in the infarcted heart of WT mice (Figure 4D). In contrast, inhibition of NO production had no effect on neovascularization after MI in AT1KO mice. These results suggest that AngII-induced eNOS activation partly regulates angiogenesis after MI.

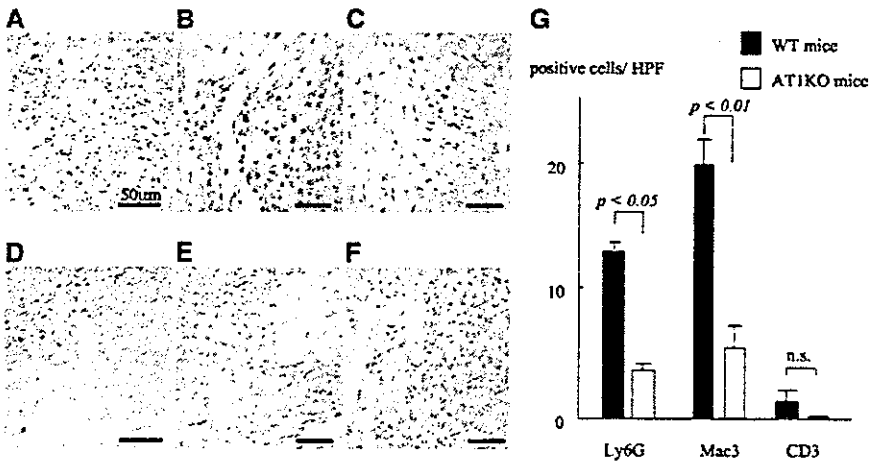

Figure 2. Cell infiltration in the myocardium at 4 days after MI. The immunohistochemical study using anti-Ly6G (granulocytes, A and D), anti-Mac3 (macrophages, B and E), and anti-CD3 (T cells, C and F) antibodies in WT mice (A, B, and C) and AT1KO mice (D, E and F). G, The number of infiltrating cells in the border zone of infarcted myocardium. Left columns show the number of Ly6G-positive cells, middle columns show the number of Mac3-positive cells, and right columns show the number of CD3-positive cells.

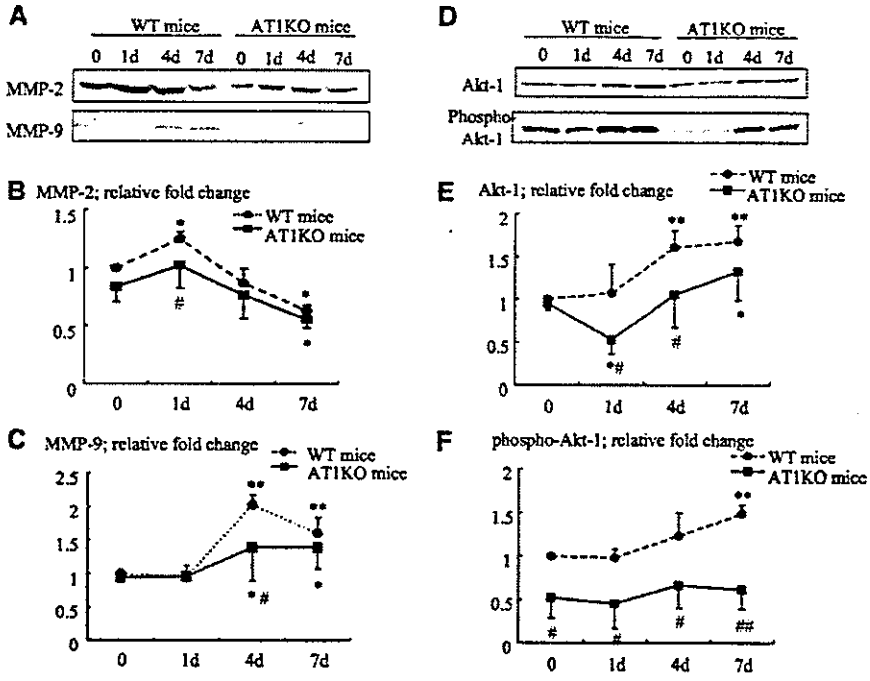

Figure 3. Protein levels of MMP-2, MMP-9, Akt-1, and phospho-Akt-1. A, Western blot analysis of MMP-2 and MMP-9 on days 0 (sham), 1, 4, and 7 after MI in WT mice and AT1KO mice. B, Relative fold change of MMP-2 protein levels. C, Relative fold change of MMP-9 protein levels. D, Western blot analysis of Akt-1 and phospho-Akt-1 on days 0 (sham), 1, 4, and 7 after MI in WT and AT1KO mice. E, Relative fold change of Akt-1 protein levels. F, Relative fold change of pospho-Akt-1 protein levels. *$P<0.05$ and **$P<0.01$ versus WT mice or AT1KO mice on day 0, #$P<0.05$ and ##$P<0.01$ versus WT mice on the same day.

AT1 Is Involved in Induction of Cytokines and Chemokines in Infarcted Myocardium

Various cytokines and chemokines have been reported to play a critical role in left ventricular remodeling after MI.[24] We examined various cytokines and chemokines using ribonuclease protection assay. The expression levels of tumor necrosis factor-α, interleukin (IL)-6, transforming growth factor (TGF)-β1, TGF-β2, TGF-β3, interferon-inducible protein-10 (IP-10), monocyte chemoattractant protein-1 (MCP-1), exotoxin, RANTES, macrophage inflammatory protein (MIP)-α, MIP-1β, and MIP-2 were increased in infarcted myocardium in WT and AT1KO mice (Figure 5A and data not shown). Most of these cytokines and chemokines such as TGF-β1, TGF-β2, TGF-β3, IP-10, MCP-1, MIP-1α, MIP-1β, and MIP-2 were more strongly upregulated in WT mice compared with AT1KO mice (Figure 5B and data not shown).

Tumor Progression Is Inhibited in AT1KO Mice

Because tumor growth depends on angiogenesis,[25] we also investigated the role of AT1 in tumor angiogenesis. The tumor size in WT mice was larger than that in AT1KO mice 14 days after implantation of sarcoma cells (Figure 6A). The much more capillaries were observed in the tumor in WT mice compared with AT1KO mice (Figure 6B and 6C). These results indicate that AngII plays an important role in angiogenesis of tumors as well as ischemic hearts.

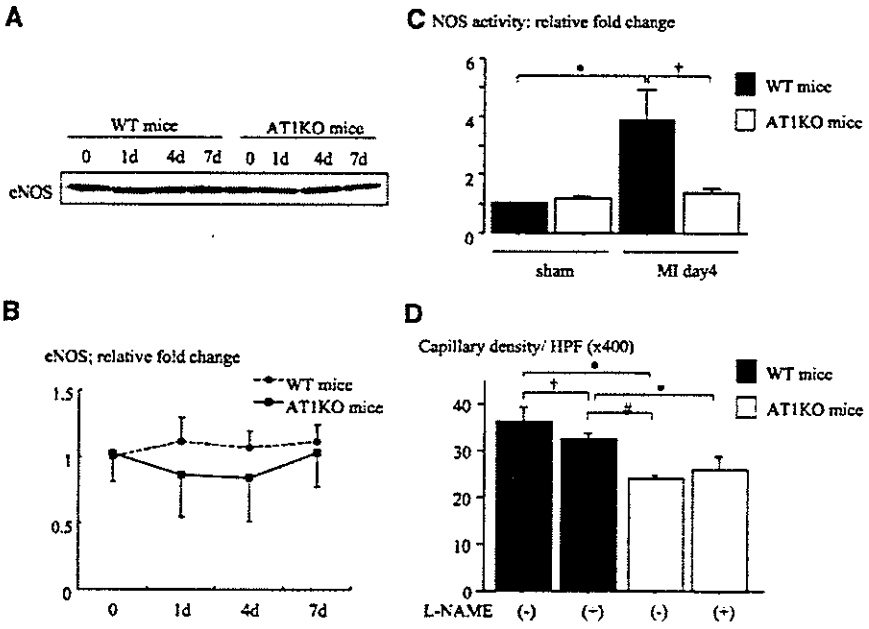

Figure 4. The effect of eNOS on angiogenesis after MI. A, Western blot analysis of eNOS on days 0 (sham), 1, 4, and 7 after MI in WT and AT1KO mice. B, Relative fold change of eNOS protein levels. C, Relative fold change of NOS activity on day 0 and day 4. *$P<0.01$ versus sham, #$P<0.05$ versus WT mice. D, Number of PECAM-positive capillaries per HPF on day 0 and day 14 after MI with or without L-NAME treatment. *$P<0.01$, #$P<0.01$, †$P<0.05$.

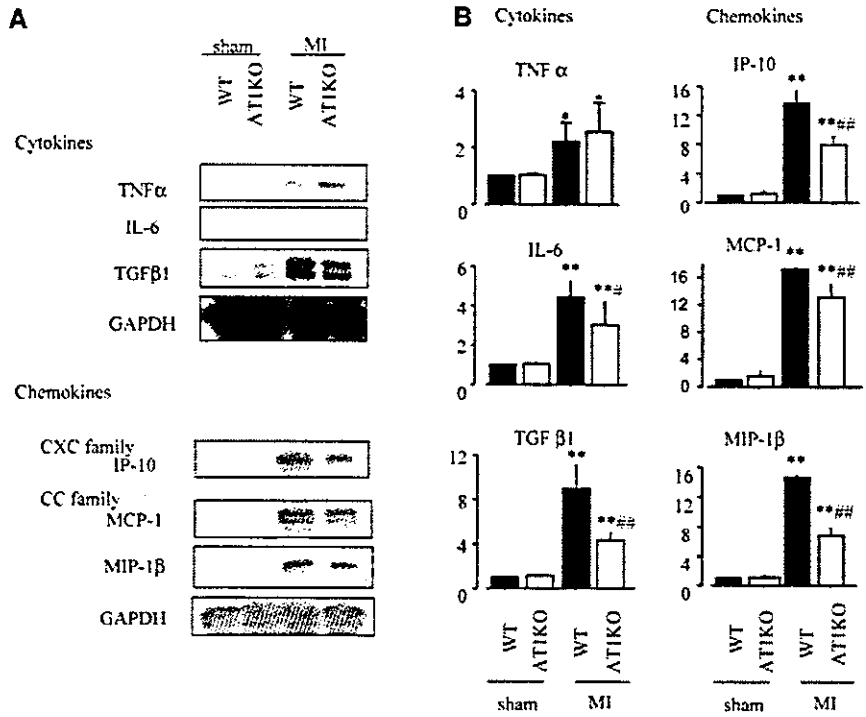

Figure 5. mRNA levels of cytokines and chemokines using RNase protection assay. A, mRNA level on day 0 (sham) and day 4 after MI in WT and AT1KO mice. B, Relative fold changes of mRNA levels. *$P<0.05$ and **$P<0.01$ versus sham, #$P<0.05$ and ##$P<0.01$ versus WT mice.

Discussion

AT1 Is Involved in Neovascularization After MI

It has been reported that an increase of neovascularization improves cardiac function and mortality,[5] and that inhibition of RAS is effective to prevent post-infarction cardiac remodeling.[1-4] It is unknown, however, whether activation of AngII/AT1 signaling induces or prevents vascularization in the infarcted heart. Some reports have demonstrated that AngII induces neovascularization in various experimental models including tumors, ischemic limb, retina, and chorioallantoic membrane.[6-8] To the contrary, there are some reports showing that inhibition of RAS induces neovascularization.[9] We thus examined in this study the role of AngII/AT1 in neovascularization during left ventricular remodeling and tumor progression using AT1KO mice. AT1KO mice exhibited less capillaries and arterioles than WT mice, suggesting that AT1 plays a pivotal role in neovascularization of the heart after MI and tumors.

AT1 Signal Plays an Important Role in Induction of MMPs and Cell Infiltration

To elucidate the molecular mechanism of how AngII induces neovascularization, we examined several molecules that have been reported to play an important role in angiogenesis. MMP-2 and MMP-9, gelatinases that digest basement membrane and play a critical role in cell invasion,[8] have been reported to be necessary for vascularization.[18,26] It has been reported that the treatment with ACE inhibitors decreases MMP-2 at mRNA and protein levels in vitro[27] and inhibits endothelial-cell migration by blocking the activity of MMP-2 and MMP-9.[26] In this study, protein levels of MMP-2 and MMP-9 were increased after MI and the increase was attenuated in AT1KO mice compared with WT mice. Histological examination revealed that infiltration of inflammatory cells such as granulocytes and macrophages was more remarkable in WT mice than AT1KO mice. These results and observations suggest that AngII induces transendothelial migration of inflammatory cells at least in part through enhanced production of MMP-2 and MMP-9. MMPs have been also demonstrated to contribute to tissue remodeling in a number of disease states, and inhibition of MMPs prevents left ventricular remodeling after MI.[28] Mice with targeted disruption of MMP-9 have attenuated ventricular remodeling and decreased cardiac rupture after infarction.[28] Our previous report also demonstrated that left ventricular dimension was

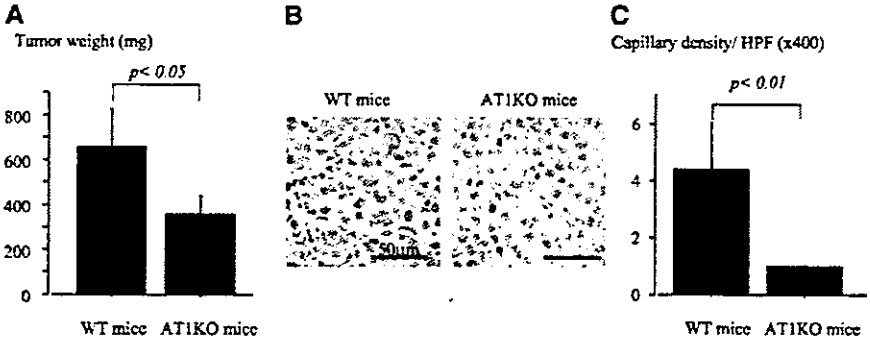

Figure 6. Tumor size and neovascularization at 14 days after sarcoma cell transplantation. A, Tumor size at 14 days after transplantation. B, The tumor was stained with anti-PECAM antibody. C, Number of PECAM-positive capillaries/HPF.

smaller in AT1KO mice than WT mice 4 weeks after MI.[4] These results suggest that MMPs activation via the AT1 signaling pathway is involved in neovascularization as well as in post-infarcted cardiac remodeling.

Activation of Akt-1 and eNOS by AngII Induces Angiogenesis in the Infarcted Myocardium

Akt plays an important role in cell survival, cell migration and angiogenesis.[29] AngII has been shown to activate Akt,[30] Akt phosphorylates, and eNOS,[20,21] thereby promoting angiogenesis. In this study, protein levels of Akt-1 were more increased in the heart of WT mice than AT1KO mice and Akt-1 was activated only in the heart of WT mice. Although there was no significant difference in protein levels of eNOS between WT mice and AT1KO mice, eNOS activity was significantly increased in WT mice compared with AT1KO mice. Moreover, the increase of capillaries in WT mice was partially inhibited by L-NAME treatment. These results suggest that AngII-induced activation of eNOS, mediated possibly by Akt, enhances angiogenesis in ischemic myocardium.

AngII Is Involved in the Production of Various Cytokines

The inflammation in cardiovascular diseases is associated with the activation of a variety of cells including lymphocytes, monocytes/macrophage, endothelial cells, smooth muscle cells, and cardiac myocytes, which express and secrete proinflammatory cytokines and chemokines.[24] These cytokines can modulate cardiac function and cardiovascular remodeling.[24] Various cytokines were increased after MI, and the increases of TGF-β, MIP-1, IP-10, and MCP-1 were more prominent in WT mice compared with AT1KO mice. These results suggest that AngII is involved in production of various cytokines after MI, which induce post-infarcted cardiac remodeling including impaired cardiac function and increased fibrosis.

Chemokines represent a family of inflammatory cytokines that induce chemotaxis of leukocyte subsets into inflammatory tissues.[31] CC-chemokines are potent chemoattractants and activators for monocytes and lymphocytes, whereas most CXC-chemokines attract neutrophils.[32] MCP-1 recruits monocytes, which produce proteolytic enzymes, reactive oxygen species, and inflammatory cytokines.[33] Recent studies have shown that neovascularization in response to tissue ischemia depends on macrophage infiltration[34] and that local infusion of MCP-1 markedly increases collateral and peripheral conductance in hindlimb ischemia model.[35] Moreover, inflammatory cytokines such as IL-1, IL-6–related cytokines, and MCP-1 have been reported to induce myocardial dysfunction[36,37] and cardiac remodeling through promotion of cardiomyocyte hypertrophy and apoptosis as well as alteration in extracellular matrix in the myocardium.[38] The MCP-1 overexpression mice showed hypertrophied left ventricular wall, dilated left ventricular dimension, and decreased cardiac function.[39] In this study, the MCP-1 expression was suppressed and the number of macrophage infiltrated into myocardium was less in AT1KO mice after MI compared with WT mice. These results and observations suggest that reduction of MCP-1 expression and macrophage infiltration might be related to less left ventricular remodeling despite less neovascularization in the heart of AT1KO mice.

AngII/AT1 signaling has 2 roles in left ventricular remodeling after MI. Activation of AT1 induces expression of chemokines and infiltration of inflammatory cells, which cause neovascularization possibly through enhanced expression of MMPs and activation of Akt. The enhanced neovascularization may prevent left ventricular remodeling by inhibition of cardiomyocyte apoptosis. However, AngII/AT1-induced cardiomyocyte hypertrophy, increased fibrosis, enhanced cytokines, and MMPs expressions induce left ventricular remodeling. Taken together with the previous reports,[4] inhibition of AngII/AT1 signal is important for preventing cardiac remodeling after MI, although it may suppress neovascularization.

Acknowledgments

We thank to E. Fujita, R. Kobayashi, A. Ohkubo, M. Watanabe, and M. Iida for technical assistant. This work was supported in part by grants from Japanese Ministry of Education, Science, Sports, and Culture and Japan Health Sciences Foundation, Takeda Medical Research Foundation, Uehara Memorial Foundation, grant-in-aid of The Japan Medical Association, The Kato Memorial Trust for Nambyo Research, and Takeda Science Foundation.

References

1. Effect of ramipril on mortality and morbidity of survivors of acute myocardial infarction with clinical evidence of heart failure. The Acute Infarction Ramipril Efficacy (AIRE) Study Investigators. *Lancet.* 1993; 342:821–828.
2. Latini R, Maggioni AP, Flather M, Sleight P, Tognoni G. ACE inhibitor use in patients with myocardial infarction. Summary of evidence from clinical trials. *Circulation.* 1995;92:3132–3137.
3. Pfeffer MA. ACE inhibition in acute myocardial infarction. *N Engl J Med.* 1995;332:118–120.
4. Harada K, Sugaya T, Murakami K, Yazaki Y, Komuro I. Angiotensin II type 1A receptor knockout mice display less left ventricular remodeling and improved survival after myocardial infarction. *Circulation.* 1999;100: 2093–2099.
5. Kocher AA, Schuster MD, Szabolcs MJ, Takuma S, Burkhoff D, Wang J, Homma S, Edwards NM, Itescu S. Neovascularization of ischemic myocardium by human bone-marrow-derived angioblasts prevents cardiomyocyte apoptosis, reduces remodeling and improves cardiac function. *Nat Med.* 2001;7:430–436.
6. Moravski CJ, Kelly DJ, Cooper ME, Gilbert RE, Bertram JF, Shahinfar S, Skinner SL, Wilkinson-Berka JL. Retinal neovascularization is prevented by blockade of the renin-angiotensin system. *Hypertension.* 2000; 36:1099–1104.
7. Sasaki K, Murohara T, Ikeda H, Sugaya T, Shimada T, Shintani S, Imaizumi T. Evidence for the importance of angiotensin II type 1 receptor in ischemia-induced angiogenesis. *J Clin Invest.* 2002;109:603–611.
8. Vu TH, Werb Z. Matrix metalloproteinases: effectors of development and normal physiology. *Genes Dev.* 2000;14:2123–2133.
9. Fabre JE, Rivard A, Magner M, Silver M, Isner JM. Tissue inhibition of angiotensin-converting enzyme activity stimulates angiogenesis in vivo. *Circulation.* 1999;99:3043–3049.
10. Kalkman EA, van Haren P, Saxena PR, Schoemaker RG. Early captopril prevents myocardial infarction-induced hypertrophy but not angiogenesis. *Eur J Pharmacol.* 1999;369:339–348.
11. Sugaya T, Nishimatsu S, Tanimoto K, Takimoto E, Yamagishi T, Imamura K, Goto S, Imaizumi K, Hisada Y, Otsuka A, Uchida H, Sugiura M, Fukuta K, Fukamizu A, Murakami K. Angiotensin II type 1a receptor-deficient mice with hypotension and hyperreninemia. *J Biol Chem.* 1995; 270:18719–18722.
12. Toko H, Zhu W, Takimoto E, Shiojima I, Hiroi Y, Zou Y, Oka T, Akazawa H, Mizukami M, Sakamoto M, Terasaki F, Kitaura Y, Takano H, Nagai T, Nagai R, Komuro I. Csx/Nkx2–5 is required for homeostasis and survival of cardiac myocytes in the adult heart. *J Biol Chem.* 2002; 277:24735–24743.

13. Harada K, Komuro I, Shiojima I, Hayashi D, Kudoh S, Mizuno T, Kijima K, Matsubara H, Sugaya T, Murakami K, Yazaki Y. Pressure overload induces cardiac hypertrophy in angiotensin II type 1A receptor knockout mice. *Circulation.* 1998;97:1952–1959.
14. Toko H, Oka T, Zou Y, Sakamoto M, Mizukami M, Sano M, Yamamoto R, Sugaya T, Komuro I. Angiotensin II type 1a receptor mediates doxorubicin-induced cardiomyopathy. *Hypertens Res.* 2002;25:597–603.
15. Wang G, Dong Z, Xu G, Yang Z, Shou C, Wang N, Liu T. The effect of antibody against vascular endothelial growth factor on tumor growth and metastasis. *J Cancer Res Clin Oncol.* 1998;124:615–620.
16. Salven P, Hattori K, Heissig B, Rafii S. Interleukin-1alpha promotes angiogenesis in vivo via VEGFR-2 pathway by inducing inflammatory cell VEGF synthesis and secretion. *FASEB J.* 2002;16:1471–1473.
17. Nicoletti A, Michel JB. Cardiac fibrosis and inflammation: interaction with hemodynamic and hormonal factors. *Cardiovasc Res.* 1999;41: 532–543.
18. Hiraoka N, Allen E, Apel IJ, Gyetko MR, Weiss SJ. Matrix metalloproteinases regulate neovascularization by acting as pericellular fibrinolysins. *Cell.* 1998;95:365–377.
19. Jiang BH, Zheng JZ, Aoki M, Vogt PK. Phosphatidylinositol 3-kinase signaling mediates angiogenesis and expression of vascular endothelial growth factor in endothelial cells. *Proc Natl Acad Sci U S A.* 2000;97: 1749–1753.
20. Dimmeler S, Fleming I, Fisslthaler B, Hermann C, Busse R, Zeiher AM. Activation of nitric oxide synthase in endothelial cells by Akt-dependent phosphorylation. *Nature.* 1999;399:601–605.
21. Fulton D, Gratton JP, McCabe TJ, Fontana J, Fujio Y, Walsh K, Franke TF, Papapetropoulos A, Sessa WC. Regulation of endothelium-derived nitric oxide production by the protein kinase Akt. *Nature.* 1999;399: 597–601.
22. Matsunaga T, Warltier DC, Weihrauch DW, Moniz M, Tessmer J, Chilian WM. Ischemia-induced coronary collateral growth is dependent on vascular endothelial growth factor and nitric oxide. *Circulation.* 2000; 102:3098–3103.
23. Murohara T, Asahara T, Silver M, Bauters C, Masuda H, Kalka C, Kearney M, Chen D, Symes JF, Fishman MC, Huang PL, Isner JM. Nitric oxide synthase modulates angiogenesis in response to tissue ischemia. *J Clin Invest.* 1998;101:2567–2578.
24. Frangogiannis NG, Smith CW, Entman ML. The inflammatory response in myocardial infarction. *Cardiovasc Res.* 2002;53:31–47.
25. Folkman J. Angiogenesis in cancer, vascular, rheumatoid and other disease. *Nat Med.* 1995;1:27–31.
26. Volpert OV, Ward WF, Lingen MW, Chesler L, Solt DB, Johnson MD, Molteni A, Polverini PJ, Bouck NP. Captopril inhibits angiogenesis and slows the growth of experimental tumors in rats. *J Clin Invest.* 1996;98: 671–679.
27. Prontera C, Mariani B, Rossi C, Poggi A, Rotilio D. Inhibition of gelatinase A (MMP-2) by batimastat and captopril reduces tumor growth and lung metastases in mice bearing Lewis lung carcinoma. *Int J Cancer.* 1999;81:761–766.
28. Heymans S, Luttun A, Nuyens D, Theilmeier G, Creemers E, Moons L, Dyspersin GD, Cleutjens JP, Shipley M, Angellilo A, Levi M, Nube O, Baker A, Keshet E, Lupu F, Herbert JM, Smits JF, Shapiro SD, Baes M, Borgers M, Collen D, Daemen MJ, Carmeliet P. Inhibition of plasminogen activators or matrix metalloproteinases prevents cardiac rupture but impairs therapeutic angiogenesis and causes cardiac failure. *Nat Med.* 1999;5:1135–1142.
29. Shiojima I, Walsh K. Role of Akt signaling in vascular homeostasis and angiogenesis. *Circ Res.* 2002;90:1243–1250.
30. Ushio-Fukai M, Alexander RW, Akers M, Yin Q, Fujio Y, Walsh K, Griendling KK. Reactive oxygen species mediate the activation of Akt/ protein kinase B by angiotensin II in vascular smooth muscle cells. *J Biol Chem.* 1999;274:22699–22704.
31. Taub DD, Oppenheim JJ. Chemokines, inflammation and the immune system. *Ther Immunol.* 1994;1:229–246.
32. Baggiolini M, Dewald B, Moser B. Interleukin-8 and related chemotactic cytokines–CXC and CC chemokines. *Adv Immunol.* 1994;55:97–179.
33. Ruiz-Ortega M, Bustos C, Hernandez-Presa MA, Lorenzo O, Plaza JJ, Egido J. Angiotensin II participates in mononuclear cell recruitment in experimental immune complex nephritis through nuclear factor-kappa B activation and monocyte chemoattractant protein-1 synthesis. *J Immunol.* 1998;161:430–439.
34. Polverini PJ, Cotran PS, Gimbrone MA, Jr., Unanue ER. Activated macrophages induce vascular proliferation. *Nature.* 1977;269:804–806.
35. Risau W. Mechanisms of angiogenesis. *Nature.* 1997;386:671–674.
36. Finkel MS, Oddis CV, Jacob TD, Watkins SC, Hattler BG, Simmons RL. Negative inotropic effects of cytokines on the heart mediated by nitric oxide. *Science.* 1992;257:387–389.
37. Yokoyama T, Vaca L, Rossen RD, Durante W, Hazarika P, Mann DL. Cellular basis for the negative inotropic effects of tumor necrosis factor-alpha in the adult mammalian heart. *J Clin Invest.* 1993;92: 2303–2312.
38. Bozkurt B, Kribbs SB, Clubb FJ, Jr., Michael LH, Didenko VV, Hornsby PJ, Seta Y, Oral H, Spinale FG, Mann DL. Pathophysiologically relevant concentrations of tumor necrosis factor-alpha promote progressive left ventricular dysfunction and remodeling in rats. *Circulation.* 1998;97: 1382–1391.
39. Kolattukudy PE, Quach T, Bergese S, Breckenridge S, Hensley J, Altschuld R, Gordillo G, Klenotic S, Orosz C, Parker-Thornburg J. Myocarditis induced by targeted expression of the MCP-1 gene in murine cardiac muscle. *Am J Pathol.* 1998;152:101–111.

Article

A novel LIM protein Cal promotes cardiac differentiation by association with CSX/NKX2-5

Hiroshi Akazawa,[1] Sumiyo Kudoh,[2] Naoki Mochizuki,[3] Noboru Takekoshi,[2] Hiroyuki Takano,[1] Toshio Nagai,[1] and Issei Komuro[1]

[1]Department of Cardiovascular Science and Medicine, Chiba University Graduate School of Medicine, Chiba 260-8670, Japan
[2]Department of Cardiology, Kanazawa Medical University, Ishikawa 920-0265, Japan
[3]Department of Structural Analysis, National Cardiovascular Center Research Institute, Osaka 565-8565, Japan

The cardiac homeobox transcription factor CSX/NKX2-5 plays an important role in vertebrate heart development. Using a yeast two-hybrid screening, we identified a novel LIM domain–containing protein, named CSX-associated LIM protein (Cal), that interacts with CSX/NKX2-5. CSX/NKX2-5 and Cal associate with each other both in vivo and in vitro, and the LIM domains of Cal and the homeodomain of CSX/NKX2-5 were necessary for mutual binding. Cal itself possessed the transcription-promoting activity, and cotransfection of Cal enhanced CSX/NKX2-5–induced activation of *atrial natriuretic peptide* gene promoter. Cal contained a functional nuclear export signal and shuttled from the cytoplasm into the nucleus in response to calcium. Accumulation of Cal in the nucleus of P19CL6 cells promoted myocardial cell differentiation accompanied by increased expression levels of the target genes of CSX/NKX2-5. These results suggest that a novel LIM protein Cal induces cardiomyocyte differentiation through its dynamic intracellular shuttling and association with CSX/NKX2-5.

Introduction

CSX/NKX2-5 is a member of NK homeobox gene family that is conserved in evolution and acts as a DNA-binding transcription activator (Komuro and Izumo, 1993; Lints et al., 1993; Akazawa and Komuro, 2003). During embryogenesis, *CSX/NKX2-5* is expressed predominantly in the heart progenitor cells from the very early stage. Targeted disruption of murine *CSX/NKX2-5* resulted in embryonic lethality due to the arrested looping morphogenesis of the heart tube (Lyons et al., 1995). In addition, mutations of *CSX/NKX2-5* cause human hereditary cardiac malformations associated with atrioventricular conduction disturbance (Schott et al., 1998). These results indicate that *CSX/NKX2-5* plays a pivotal role in normal heart development in mammals.

To understand the mechanisms of how *CSX/NKX2-5* controls cardiac development, it is necessary to elucidate the molecular framework of fine-tuned transcriptional regulation of its distinct target genes. Recently, protein–protein interactions have been recognized to be important in many biological processes. Protein complexes consisting of transcription factors and cofactors are responsible for transcriptional regulation, and its composition is thought to be the key determinant of specificity and intensity of the reaction. Transcriptional activity of CSX/NKX2-5 is modulated through physical interaction with other transcription factors such as GATA-4 (Durocher et al., 1997; Lee et al., 1998; Shiojima et al., 1999), SRF (Chen and Schwartz, 1996), and Tbx-5 (Bruneau et al., 2001; Hiroi et al., 2001). Here, we isolated a novel CSX/NKX2-5–associated protein by a yeast two-hybrid screening using *CSX/NKX2-5* as a bait. The protein was a novel LIM domain–containing protein, which we named CSX-associated LIM protein (*Cal*). The LIM domain is a double-zinc finger motif and functions as a module for protein–protein interactions (Dawid et al., 1998; Bach, 2000). Nuclear LIM proteins such as LIM homeodomain proteins and LIM only proteins are directly involved in transcriptional regulation during cell differentiation (Dawid et al., 1998; Bach, 2000). Cytoplasmic LIM proteins are involved in divergent biological processes such as regulation of cytoarchitecture, protein trafficking, and specification of cell polarity (Dawid et al., 1998; Bach,

Address correspondence to Issei Komuro, Dept. of Cardiovascular Science and Medicine, Chiba University Graduate School of Medicine, 1-8-1 Inohana, Chuo-ku, Chiba 260-8670, Japan. Tel.: 81-43-226-2097. Fax: 81-43-226-2557. email: komuro-tky@umin.ac.jp

Key words: cardiogenesis; homeobox transcription factor; LIM domain; nucleocytoplasmic transport; transcriptional regulation

Abbreviations used in this paper: ANP, atrial natriuretic peptide; Ca^{2+}, calcium; Cal, CSX-associated LIM protein; CRP, cysteine-rich protein; LMB, leptomycin B; LPP, lipoma preferred partner; NES, nuclear export signal; SERCA2, sarcoplasmic reticulum Ca^{2+}-ATPase 2; trip6, thyroid receptor interacting protein 6.

The Journal of Cell Biology, Volume 164, Number 3, February 2, 2004 395–405
http://www.jcb.org/cgi/doi/10.1083/jcb.200309159

2000). In regard to muscle development, the roles of cysteine-rich protein (CRP) 3/MLP, which is primarily cytoplasmic, have attracted much attention (Arber et al., 1994). Overexpression of CRP3/MLP in C2C12 myoblasts promoted skeletal myogenesis, whereas inhibition of CRP3/MLP activity by antisense oligonucleotide interrupted terminal differentiation of these cells. Mice homozygous for CRP3/MLP mutation exhibited dilated cardiomyopathy resulted from disrupted cytoarchitecture in cardiomyocytes (Arber et al., 1997). These results indicate the possibility that cytoplasmic LIM proteins regulate cell differentiation as well. Recently, some cytoplasmic LIM proteins have been reported to show nuclear localization. For example, CRP3/MLP associates with nuclear LIM proteins Lmo1 and Apterous (Arber and Caroni, 1996) and basic helix-loop-helix transcription factor MyoD (Kong et al., 1997) as well as cytoskeletal proteins, Zyxin, and α actinin (Louis et al., 1997). However, the molecular mechanism by which the cytoplasmic LIM proteins are involved in nuclear events remains largely unknown.

Here, we show that Cal functions as a coactivator for CSX/NKX2-5 and fulfills its cooperative function based on its dynamic intracellular shuttling mechanisms. Consistent with the notion that the LIM domains function as an interface of protein–protein interactions, the LIM domains of Cal are required for binding to the homeodomain of CSX/NKX2-5. Cal itself has the transcription-promoting activity and activates the *atrial natriuretic peptide* (*ANP*) promoter by forming complex with CSX/NKX2-5. Cal traffics out of the nucleus by nuclear export signal (NES)–dependent mechanisms and traffics into the nucleus in response to an increase of intracellular calcium (Ca^{2+}) concentration. Nuclear expression of Cal promotes cardiac differentiation of P19CL6 cells in vitro. Characterization of complex formation between CSX/NKX2-5 and Cal will provide a unique framework whereby gene expression during cardiogenesis is fine-tuned by the primarily cytoplasmic LIM proteins that were supposed to be involved in cytoskeletal organization.

Results

Molecular cloning and characterization of Cal

To identify proteins that interact with CSX/NKX2-5, we screened a human heart library by the yeast two-hybrid system using the full length of *CSX/NKX2-5* as a bait, and isolated a gene out of 25 positive clones, which we named *Cal*. Using the human Cal cDNA, we isolated the mouse full-length *Cal* cDNA, which encodes a protein of 375 aa (Fig. 1 A) with three tandemly arrayed LIM domains in the COOH terminus. It contains a region abundant in proline residues in the NH_2 terminus. In addition, there is a leucine-rich motif that matches the consensus sequence for NES. These salient structural features are shared among Zyxin family of LIM domain–containing proteins consisting of *Zyxin* (Beckerle, 1997), *lipoma preferred partner* (*LPP*) (Petit et al., 1996), *Ajuba* (Goyal et al., 1999), and *thyroid receptor interacting protein 6 (trip6;* Yi and Beckerle, 1998). Northern blot analysis revealed that there were two transcripts of different sizes, 3.2 and 6.0 kb, and that Cal was highly expressed in a variety of tissues (Fig. 1 B). Most abundant expression was observed in the heart and relatively abundant expression was observed in the lung, intestine, and uterus, whereas little transcript was detected in the brain and liver. RNA in situ hybridization studies revealed that *Cal* was ex-

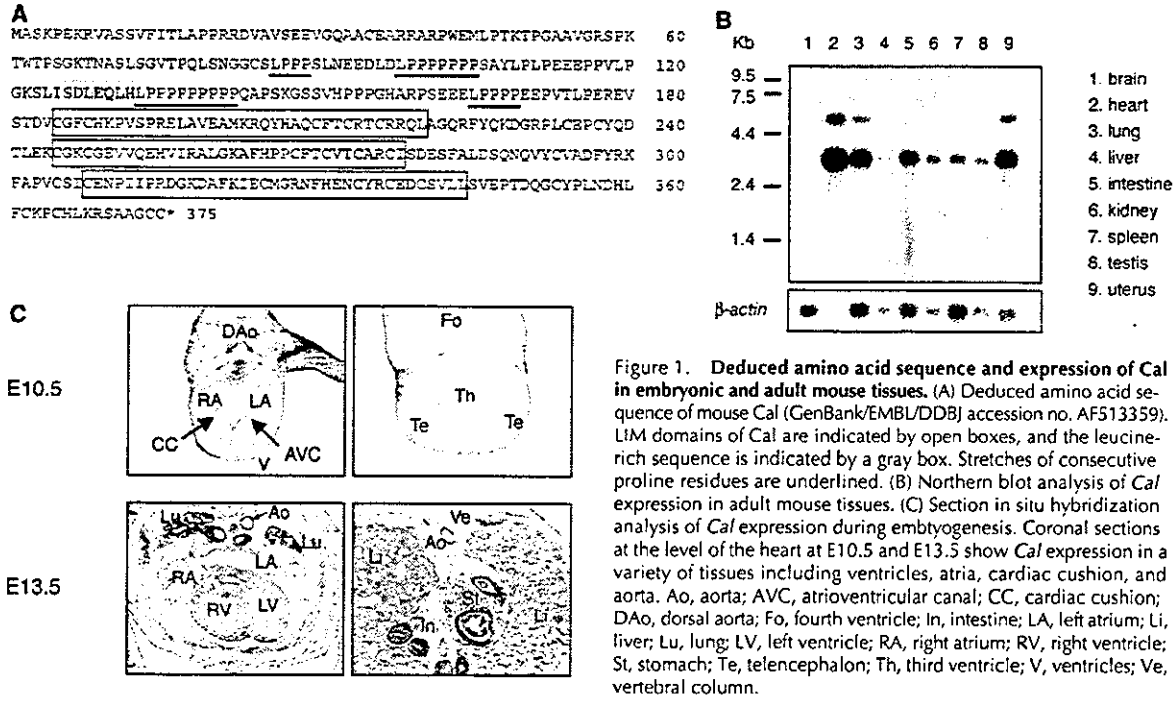

Figure 1. **Deduced amino acid sequence and expression of Cal in embryonic and adult mouse tissues.** (A) Deduced amino acid sequence of mouse Cal (GenBank/EMBL/DDBJ accession no. AF513359). LIM domains of Cal are indicated by open boxes, and the leucine-rich sequence is indicated by a gray box. Stretches of consecutive proline residues are underlined. (B) Northern blot analysis of *Cal* expression in adult mouse tissues. (C) Section in situ hybridization analysis of *Cal* expression during embtyogenesis. Coronal sections at the level of the heart at E10.5 and E13.5 show *Cal* expression in a variety of tissues including ventricles, atria, cardiac cushion, and aorta. Ao, aorta; AVC, atrioventricular canal; CC, cardiac cushion; DAo, dorsal aorta; Fo, fourth ventricle; In, intestine; LA, left atrium; Li, liver; Lu, lung; LV, left ventricle; RA, right atrium; RV, right ventricle; St, stomach; Te, telencephalon; Th, third ventricle; V, ventricles; Ve, vertebral column.

pressed in a wide variety of cell-lineages including the heart, lung, and intestine during mouse embryogenesis (Fig. 1 C). Lesser transcript was observed in the liver, and no transcript was observed in the vertebral column and encephalon.

Cal forms a complex with CSX/NKX2-5

To examine whether CSX/NKX2-5 and Cal directly interact with each other in vivo, we cotransfected COS7 cells with HA-tagged CSX/NKX2-5 and FLAG-tagged Cal. Cell lysates were subjected to immunoprecipitation using anti-FLAG antibody, and coprecipitating CSX/NKX2-5 was detected by immunoblotting with anti-HA antibody (Fig. 2 A). This result suggests that CSX/NKX2-5 and Cal associate with each other in mammalian cells as well as yeast cells.

Next, to confirm the direct interaction between CSX/NKX2-5 and Cal, and if so, to determine the domain responsible for the association, GST pull-down assays were performed with GST-Cal fusion protein and in vitro–translated CSX/NKX2-5. GST-Cal immobilized on glutathione-Sepharose beads retained in vitro–translated CSX/NKX2-5, indicating the direct interaction between CSX/NKX2-5 and Cal (Fig. 2 B). A CSX/NKX2-5 mutant lacking the homeodomain did not associate with Cal, but the homeodomain of CSX/NKX2-5 was enough for association (Fig. 2 B). These results suggest that the homeodomain of CSX/NKX2-5 is necessary and sufficient for the interaction with Cal. We also examined the binding of GST-CSX/NKX2-5 and in vitro–translated Cal and its mutants. A Cal mutant lacking all three LIM domains did not associate with CSX/NKX2-5, but Cal mutants containing at least two LIM domains did associate with CSX/NKX2-5 (Fig. 2 C). These results suggest that the LIM domains of Cal are responsible for interaction with CSX/NKX2-5.

CSX/NKX2-5 and Cal synergistically transactivate the ANP promoter

To examine the effect of Cal on transcriptional activity of CSX/NKX2-5, we performed a series of reporter assays using the luciferase reporter linked to the *ANP* promoter. When the luciferase construct containing the *ANP* promoter was cotransfected with CSX/NKX2-5 expression vector, significant fold induction of the promoter activity was observed as reported previously (Shiojima et al., 1999). Although overexpression of Cal had no effect on the *ANP* promoter, cotransfection of Cal with CSX/NKX2-5 induced much stronger transactivation than CSX/NKX2-5 alone, suggesting that CSX/NKX2-5 and Cal synergistically transactivate the *ANP* promoter (Fig. 3 A). CSX/NKX2-5 and Cal also synergistically transactivated the luciferase construct containing multimerized CSX/NKX2-5–binding sites (Fig. 3 A).

Next, we examined whether the interaction between CSX/NKX2-5 and Cal was required for the synergistic

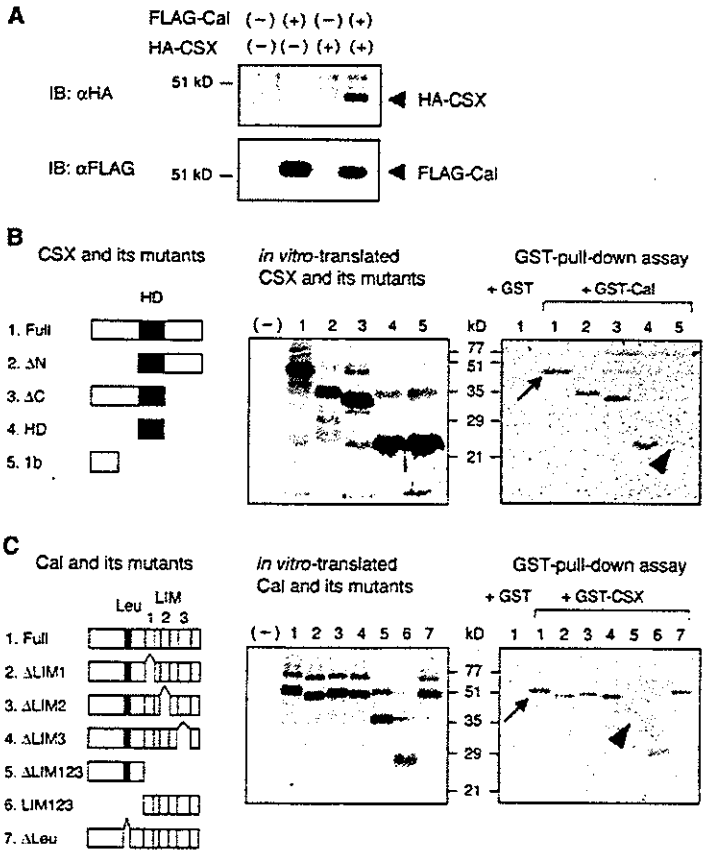

Figure 2. **Complex formation between CSX/NKX2-5 and Cal.** (A) Coimmunoprecipitation of CSX/NKX2-5 and Cal in transfected COS7 cells. Immunoprecipitates with anti-FLAG antibody were separated by SDS-PAGE and immunoblotted with anti-HA antibody (top). The same blot was reprobed with anti-FLAG antibody to confirm the presence of FLAG-tagged Cal (bottom). (B) GST pull-down assay for mapping of a region in CSX/NKX2-5 required for binding to Cal. In vitro–translated CSX/NKX2-5 and its mutants labeled with ^{35}S were incubated with GST-Cal immobilized on glutathione-Sepharose beads, and bound proteins were separated by SDS-PAGE and visualized by autoradiography. The arrow indicates the CSX/NKX2-5 protein bound to GST-Cal. A CSX/NKX2-5 mutant lacking the homeodomain did not associate with Cal (arrowhead), whereas a CSX/NKX2-5 mutant containing only the homeodomain did associate. HD, homeodomain. (C) GST pull-down assay for mapping of a region in Cal required for binding to CSX/NKX2-5. In vitro–translated Cal and its mutants labeled with ^{35}S were incubated with GST-CSX/NKX2-5. The arrow indicates the Cal protein bound to GST-CSX/NKX2-5. A Cal mutant lacking all the LIM domains did not associate with CSX/NKX2-5 (arrowhead), whereas a Cal mutant containing only the LIM domains did associate.

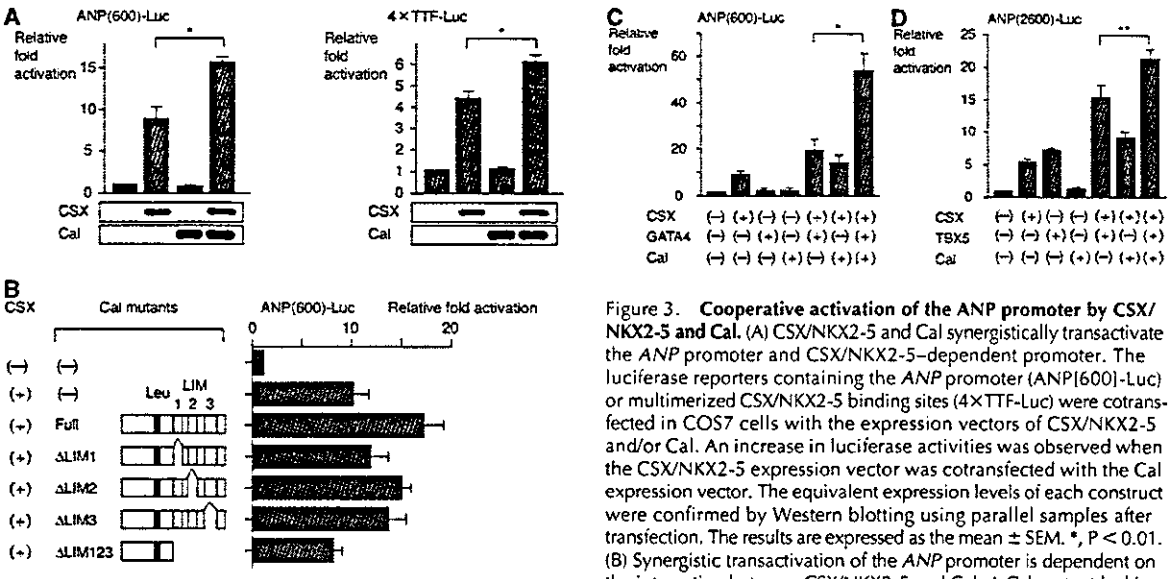

Figure 3. **Cooperative activation of the ANP promoter by CSX/NKX2-5 and Cal.** (A) CSX/NKX2-5 and Cal synergistically transactivate the *ANP* promoter and CSX/NKX2-5–dependent promoter. The luciferase reporters containing the *ANP* promoter (ANP[600]-Luc) or multimerized CSX/NKX2-5 binding sites (4×TTF-Luc) were cotransfected in COS7 cells with the expression vectors of CSX/NKX2-5 and/or Cal. An increase in luciferase activities was observed when the CSX/NKX2-5 expression vector was cotransfected with the Cal expression vector. The equivalent expression levels of each construct were confirmed by Western blotting using parallel samples after transfection. The results are expressed as the mean ± SEM. *, $P < 0.01$. (B) Synergistic transactivation of the *ANP* promoter is dependent on the interaction between CSX/NKX2-5 and Cal. A Cal mutant lacking all three LIM domains, the docking module for binding to CSX/NKX2-5, exhibited no significant cooperation on CSX/NKX2-5–induced promoter activation. The results are expressed as the mean ± SEM. (C) Cal augments synergistic transactivation between CSX/NKX2-5 and GATA-4. COS7 cells were cotransfected with the luciferase reporter containing the *ANP* promoter (ANP[600]-Luc) and the expression vectors of CSX/NKX2-5 and/or GATA-4 and/or Cal. Cotransfection with CSX/NKX2-5 and GATA-4 exhibited synergistic transactivation, that was further enhanced by additional expression of Cal. The results are expressed as the mean ± SEM. *, $P < 0.01$. (D) Cal augments synergistic transactivation between CSX/NKX2-5 and Tbx-5. Cotransfection with CSX/NKX2-5 and Tbx-5 exhibited synergistic transactivation of the *ANP* promoter (ANP[2600]-Luc), that was further augmented by additional expression of Cal. The results are expressed as the mean ± SEM. **, $P < 0.05$.

transactivation of the *ANP* promoter. Although Cal mutants lacking one LIM domain, which retain the ability to bind to CSX/NKX2-5, showed synergistic activation with CSX/NKX2-5 on the *ANP* promoter, the Cal mutant lacking the three LIM domains, which does not bind to CSX/NKX2-5, exhibited no significant cooperation on CSX/NKX2-5–induced promoter activation (Fig. 3 B). These results suggest that the synergistic transactivation was dependent on the mutual binding between CSX/NKX2-5 and Cal.

It has been reported that CSX/NKX2-5 and a zinc-finger transcription factor, GATA-4, display synergistic transcriptional activation of the *ANP* promoter (Durocher et al., 1997; Lee et al., 1998; Shiojima et al., 1999). As shown in Fig. 3 C, Cal augmented this synergistic promoter activation between CSX/NKX2-5 and GATA4. We and others reported recently that CSX/NKX2-5 and a T-box transcription factor, Tbx-5, showed synergistic transcriptional activation of the *ANP* promoter (Bruneau et al., 2001; Hiroi et al., 2001). Cal also augmented this synergistic promoter activation between CSX/NKX2-5 and Tbx-5 (Fig. 3 D).

Cal is a transactivator

To understand how Cal exhibits synergistic transcriptional activation with CSX/NKX2-5, we examined the transcriptional activity of Cal. The expression vector containing Cal fused to GAL4 DNA-binding domain was cotransfected in COS7 cells with the luciferase reporter containing the multimerized GAL4-binding sites. As shown Fig. 4, full length of Cal fused to the DNA-binding domain of GAL4 transactivated a GAL4-dependent reporter ~13.0-fold compared with DNA-binding domain of GAL4 alone. Cal mutants lacking all three LIM domains, LIM2 or LIM3 domains showed no transcriptional activity, whereas the Cal mutant containing only LIM2 and LIM3 domains showed stronger activity than the full length of Cal. Deletion of LIM1 domain showed even stronger activity, suggesting that Cal itself has the transcription-promoting activity and that its transactivation domain is localized

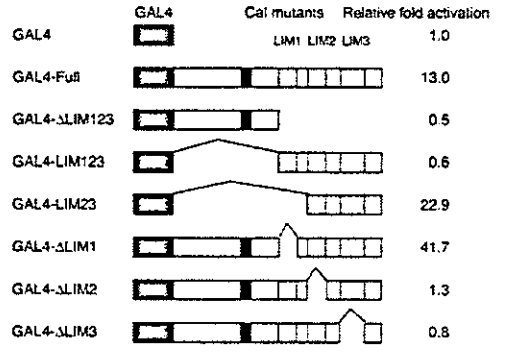

Figure 4. **Transcriptional activity of Cal.** Expression vectors encoding the GAL4 DNA binding domain fused to the indicated regions of Cal were transiently transfected into COS7 cells with the pG5luc-luciferase reporter, which contained five GAL4 binding sites. Cal fused to the DNA binding domain of GAL4 significantly transactivated a GAL4-dependent reporter, indicating that Cal possesses transcriptional activity. Cal mutants lacking LIM2 or LIM3 showed no transcriptional activity, whereas Cal mutants containing LIM2 and LIM3 showed stronger activity.

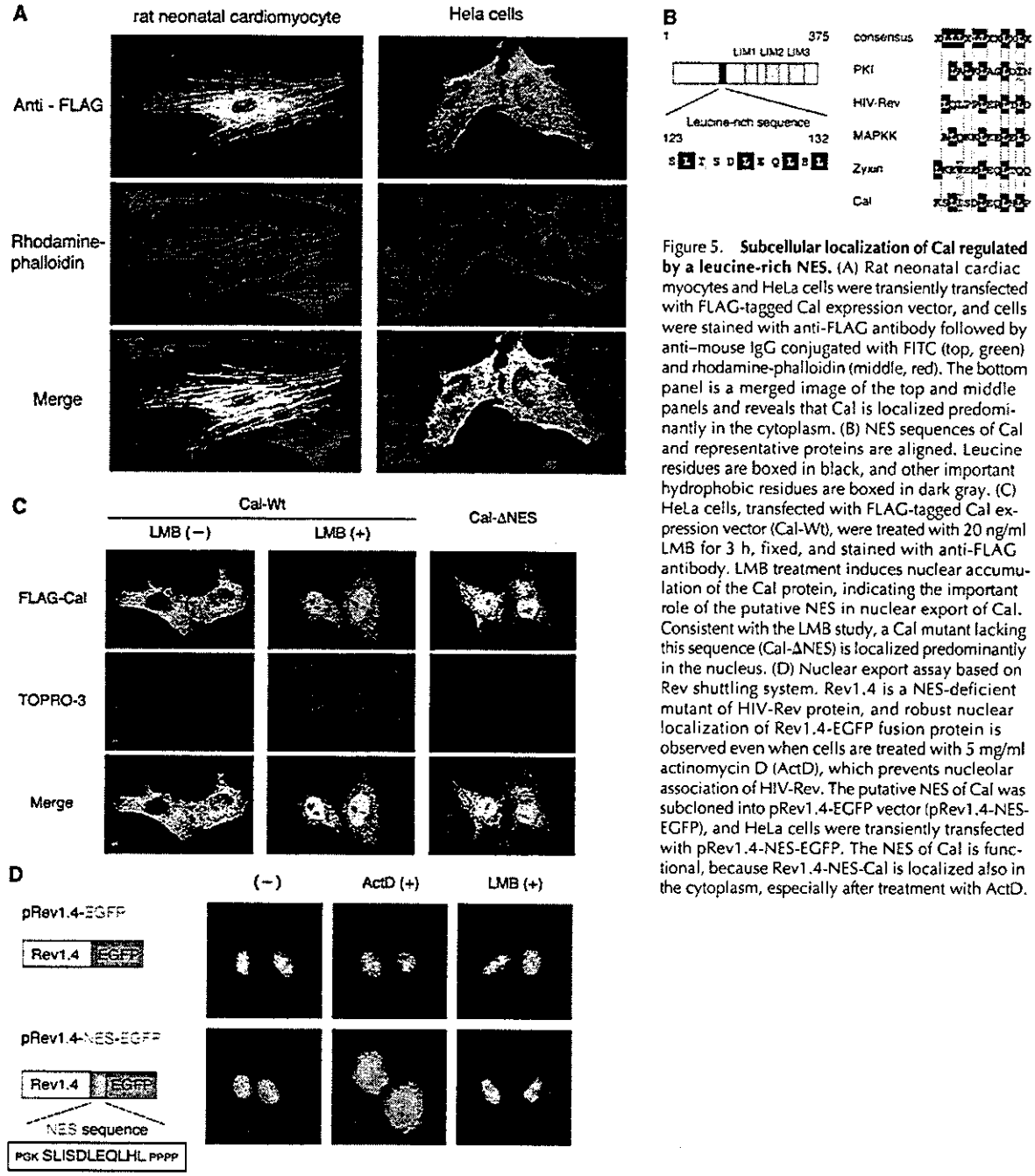

Figure 5. **Subcellular localization of Cal regulated by a leucine-rich NES.** (A) Rat neonatal cardiac myocytes and HeLa cells were transiently transfected with FLAG-tagged Cal expression vector, and cells were stained with anti-FLAG antibody followed by anti-mouse IgG conjugated with FITC (top, green) and rhodamine-phalloidin (middle, red). The bottom panel is a merged image of the top and middle panels and reveals that Cal is localized predominantly in the cytoplasm. (B) NES sequences of Cal and representative proteins are aligned. Leucine residues are boxed in black, and other important hydrophobic residues are boxed in dark gray. (C) HeLa cells, transfected with FLAG-tagged Cal expression vector (Cal-Wt), were treated with 20 ng/ml LMB for 3 h, fixed, and stained with anti-FLAG antibody. LMB treatment induces nuclear accumulation of the Cal protein, indicating the important role of the putative NES in nuclear export of Cal. Consistent with the LMB study, a Cal mutant lacking this sequence (Cal-ΔNES) is localized predominantly in the nucleus. (D) Nuclear export assay based on Rev shuttling system. Rev1.4 is a NES-deficient mutant of HIV-Rev protein, and robust nuclear localization of Rev1.4-EGFP fusion protein is observed even when cells are treated with 5 mg/ml actinomycin D (ActD), which prevents nucleolar association of HIV-Rev. The putative NES of Cal was subcloned into pRev1.4-EGFP vector (pRev1.4-NES-EGFP), and HeLa cells were transiently transfected with pRev1.4-NES-EGFP. The NES of Cal is functional, because Rev1.4-NES-Cal is localized also in the cytoplasm, especially after treatment with ActD.

within the LIM2 and LIM3 domains, whereas LIM1 may function as a repressor domain.

Cal is predominantly localized in the cytoplasm and shuttles between the cytoplasm and the nucleus

We examined the subcellular localization of Cal protein in cultured cells. Cultured cardiac myocytes of neonatal rats were transiently transfected with FLAG-tagged Cal expression vector, and immunofluorescence analysis was performed using anti-FLAG antibody. Cal protein was predominantly localized in the cytoplasm of cardiac myocytes at steady state (Fig. 5 A). Similar pattern of immunofluorescence was obtained in other cell lines such as HeLa (Fig. 5 A), COS7, and NIH3T3 cells (not depicted).

Within the amino acid sequence of Cal, there was a leucine-rich sequence that matched the consensus sequence of NES (Fig. 5 B). During a nuclear export cycle, an exportin molecule CRM1 recognizes the NES and forms a complex

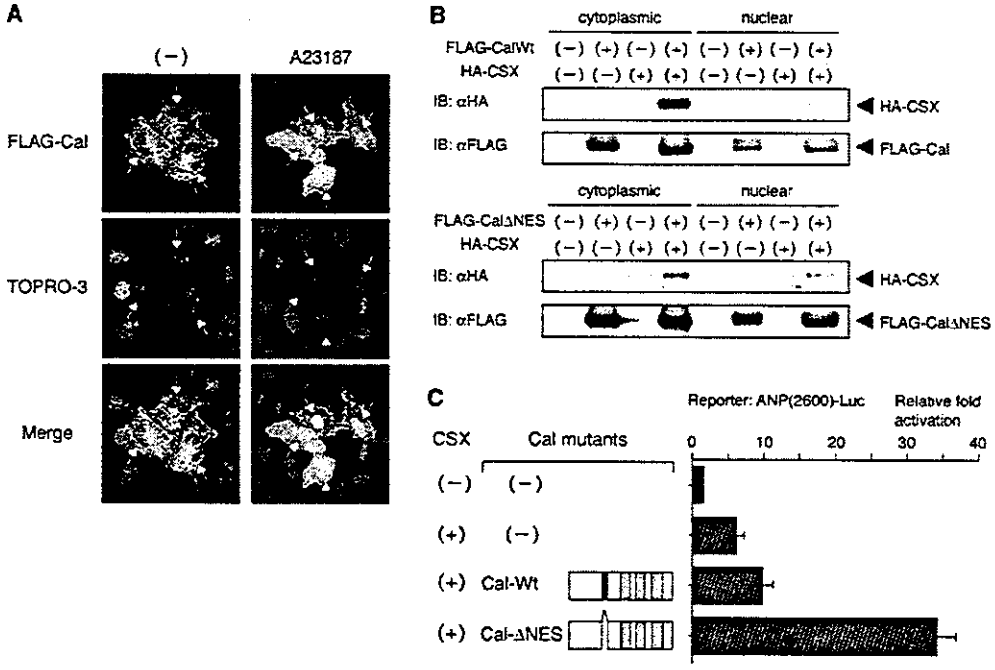

Figure 6. **Nuclear transport of Cal in response to calcium ionophore and implications of nuclear accumulation of Cal in transcriptional cooperativity with CSX/NKX2-5.** (A) HeLa cells, transfected with FLAG-tagged Cal expression vector, were treated with vehicle or calcium ionophore A23187 (2 μM) for 15 min, fixed, and stained with anti-FLAG antibody. Nuclear accumulation of Cal is observed in significant portions of transfected cells after treatment with A23187. The arrows indicate the nuclei of the transfected cells. (B) Coimmunoprecipitation of CSX/NKX2-5 and Cal (Cal-Wt) or nuclear form of Cal (Cal-ΔNES) in preparations of cytoplasmic or nuclear fractions of transfected COS7 cells. Cal-ΔNES showed significantly stronger interaction with CSX/NKX2-5 in the nucleus than Cal-Wt. (C) The luciferase reporter containing the *ANP* promoter was cotransfected in COS7 cells with the expression vectors of CSX/NKX2-5 and Cal-Wt or Cal-ΔNES. Cal-ΔNES showed much stronger synergistic activation with CSX/NKX2-5 than Cal-Wt. The results are expressed as the mean ± SEM.

with RanGTP, and mediates transport to the cytoplasm (Fornerod et al., 1997; Mattaj and Englmeier, 1998; Ohno et al., 1998; Kuersten et al., 2001). NES-dependent nuclear export is inhibited by leptomycin B (LMB) that interferes with the binding of CRM1 to NES (Kudo et al., 1998). Inhibition of CRM1-dependent nuclear export using LMB resulted in rapid nuclear accumulation of Cal protein in HeLa cells (Fig. 5 C). Although immunofluorescence studies indicated that the main compartment where Cal is localized at steady state was the cytoplasm, the accumulation of CAL after treatment with LMB suggested that Cal can shuttle between the cytoplasm and the nucleus.

To confirm that the putative NES contributes to nuclear export of Cal, we deleted the NES sequence (residues 123–132) in the FLAG-tagged Cal expression vector (Cal-ΔNES) and examined the subcellular localization of Cal-ΔNES mutant. Cal-ΔNES was predominantly localized in the nucleus (Fig. 5 C), suggesting that this sequence mediates the CRM1-dependent nuclear export of Cal. To test this sequence of Cal functions as an NES, we introduced this sequence into the export-deficient form of Rev-EGFP, and tested its nuclear export activity in HeLa cells. The putative NES of Cal displayed the export activity, especially in the presence of actinomycin D, which prevents nucleolar association of Rev protein (Fig. 5 D). These results indicate that this 123-132–amino acid sequence of Cal really functions as an NES.

Cal shuttles into the nucleus in response to Ca^{2+} signal

We explored a specific signal capable of targeting Cal protein to the nucleus. When intracellular Ca^{2+} levels were increased by Ca^{2+} ionophore A23187, Cal protein was transported to the nucleus (Fig. 6 A). Nuclear accumulation of Cal was detected at 10 min after addition of A23187. No other cellular signals possessed ability to transport Cal into the nucleus. For example, treatment with cytochalasin D, an actin filament disrupting reagent, tetradecanoylphorbol 13-acetate, PKC activator, forskolin, an adenylate cyclase activator, anisomycin, Jun-NH_2–terminal kinase agonist, okadaic acid, a serine/threonine phosphatase inhibitor did not induce nuclear translocation of Cal protein.

Next, we examined whether nucleocytoplasmic shuttling of Cal protein had important implications for modifying the transcriptional activity of CSX/NKX2-5. As indicated by coimmunoprecipitation experiments by using cytoplasmic and nuclear fractions of transfected cells, interaction between CSX/NKX2-5 and wild-type of Cal (Cal-Wt) was detectable predominantly in the cytoplasm and slightly in the nucleus (Fig. 6 B). When Cal-ΔNES, which lacks the NES and is predominantly localized in the nucleus, was cotransfected, the level of coprecipitating CSX/NKX2-5 in the nuclear fraction increased significantly (Fig. 6 B). Furthermore, Cal-ΔNES showed much stronger synergistic transactivation of the *ANP* promoter than Cal-Wt, when cotransfected with CSX/

NKX2-5 (Fig. 6 C). These results suggest that nuclear translocation of Cal enhances CSX/NKX2-5–induced promoter activation by promoting mutual interaction in the nucleus.

Nuclear accumulation of Cal induces cardiac differentiation of P19CL6 cells

To determine whether synergistic transactivation by Cal has a significant effect on cardiomyocyte differentiation, we isolated P19CL6 clones, which stably overexpress wild-type Cal (P19CL6-CAL-Wt) or Cal mutant lacking the NES (P19CL6-Cal-ΔNES). When cultured in the medium containing 1% DMSO, P19CL6 cells differentiated into cardiomyocytes, which exhibit spontaneous beating and express cardiac-specific genes (Monzen et al., 1999). The expression of cardiac-specific genes was examined in P19CL6 cells, P19CL6-Cal-Wt, and P19CL6-Cal-ΔNES during differentiation (Fig. 7 A). Northern blot analysis revealed that expression levels of a cardiac transcription factor *GATA-4* and *sarcoplasmic reticulum Ca^{2+}-ATPase 2* (*SERCA2*) as well as *connexin 43* and *calreticulin*, known as downstream targets for CSX/NKX2-5, were increased in P19CL6-Cal-ΔNES cells. RT-PCR analysis revealed that expression of *ANP* gene was also up-regulated in P19CL6-Cal-ΔNES cells, which was consistent with the results that Cal augmented *ANP* promoter activation induced by CSX/NKX2-5. Immunocytochemical analysis revealed that in P19CL6-Cal-ΔNES, a larger number of cells were stained positive with anticardiac troponin T antibody than the parental P19CL6 cells (Fig. 7 B), suggesting that nuclear accumulation of Cal strongly promotes cardiac differentiation.

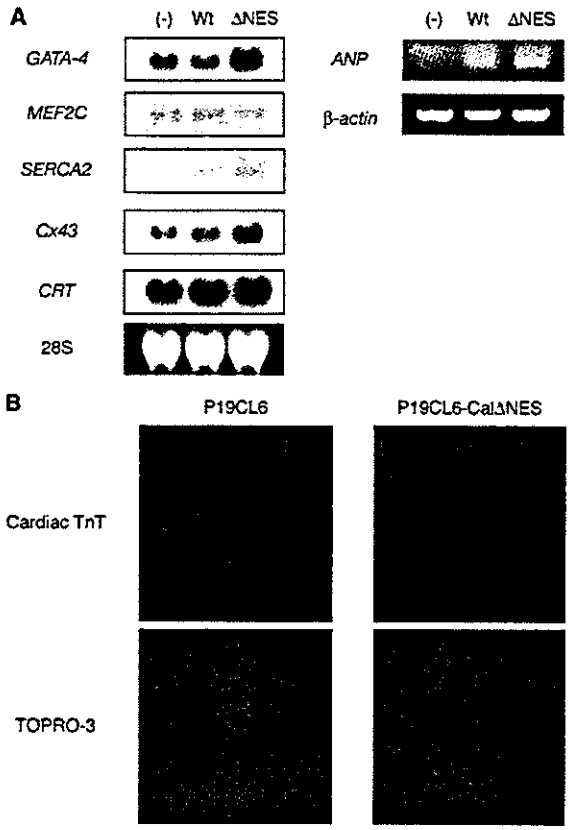

Figure 7. **Promotion of cardiac differentiation in P19CL6 cells by nuclear accumulation of Cal.** (A) Expression of cardiac genes was examined on differentiation day nine of P19CL6 cells, P19CL6 cells stably expressing Cal-Wt and Cal-ΔNES. Northern blot analysis was performed with *GATA-4, MEF2C, SERCA2, Connexin43 (Cx43)*, and *calreticulin (CRT)* cDNAs and RT-PCR was performed using specific primers for *ANP*. Notably, expression levels of target genes for CSX/NKX2-5 such as *Cx43, CRT*, and *ANP* were increased in P19CL6-Cal-ΔNES. (B) Cardiac differentiation in P19CL6 cells on differentiation day 14 was determined by immunofluorescence with anticardiac troponin T (TnT) antibody. Much larger number of cells were stained positive for cardiac TnT in P19CL6-Cal-ΔNES.

Discussion

Cal is a novel LIM domain–containing protein

We identified a novel protein Cal, which associates with the cardiac homeobox transcription factor CSX/NKX2-5. *Cal* is a member of Zyxin family, that commonly have a proline-rich region at the NH_2 terminus, a leucine-rich sequence, and three tandem LIM domains located at the COOH terminus. The proline-rich regions of Zyxin serve as interface to bind to SH3 domain of Vav (Hobert et al., 1996) and EVH1 domain of Ena/VASP family proteins (Renfranz and Beckerle, 2002) that are implicated in control of actin organization (Gertler et al., 1996). LPP also contains proline-rich motifs that are required for the interaction with the EVH1 domain (Prehoda et al., 1999). This proline-rich region of LPP directly interacts with VASP in vitro, and LPP is colocalized with VASP in the focal adhesion. The proline-rich regions of Ajuba interact with Grb2 (Goyal et al., 1999). Expression of Ajuba enhances MAPK activity in fibroblasts and promotes meiotic maturation of *Xenopus* oocytes through activation of MAPK in Grb2- and Ras-dependent manner (Goyal et al., 1999). The NH_2-terminal portion of *Cal* also contains stretches of proline-rich sequences. Especially, two proline-rich sequences (LPPPPPPP 98-105 and LPPPPPPPPP 133-142) of Cal lead us to speculate that Cal might associate with profilin and be involved in the organization of cytoskeletal actin in the cytoplasm because the sequence of consecutive prolines flanked by leucine has been thought to be a ligand motif for profilin (Mahoney et al., 1997). Identification of proteins binding to the proline-rich region of Cal would provide further insights into its cellular function.

Cal interacts with CSX/NKX-2.5 both in vitro and in vivo

GST pull-down assays and coimmunoprecipitation experiments indicated the association of Cal with CSX/NKX2-5 both in vitro and in vivo. Analyses using mutants of both proteins revealed that the mutual binding was mediated through the homeodomain of CSX/NKX2-5 and the LIM domains of Cal. Besides binding to DNA, the homeodomain of CSX/NKX2-5 acts as a module for the interaction with its binding partner such as GATA-4 (Durocher et al., 1997; Lee et al., 1998; Shiojima et al., 1999), SRF (Chen and Schwartz, 1996), and Tbx-5 (Hiroi et al., 2001). The LIM domains of Cal have a cysteine-histidine rich, double zinc-finger motif that functions as a protein–protein in-

teraction module (Dawid et al., 1998; Bach, 2000). The LIM domains of Zyxin interact with members of CRP family (Sadler et al., 1992) and serine/threonine kinase h-warts/LATS1 (Hirota et al., 2000). During mitosis, phosphorylation of Zyxin by Cdc2 promotes the binding between Zyxin and h-warts/LATS1, and the complex is targeted to the mitotic apparatus. The possibility that interaction between CSX/NKX2-5 and Cal is modulated by specific protein modification remains to be determined.

Abundant expression of *Cal* was detected in the heart during embryogenesis and maintained in the atrial and ventricular chambers through the adulthood. *Cal* was also expressed in a variety of tissues such as the aorta, lung, and intestine, but little expression was detected in the brain and liver. Although the functional roles of Cal in tissues other than the heart remain unknown at present, Cal may associate with other NK homeobox transcription factors, because the amino acid sequences of homeodomains, which are responsible for binding to Cal, are highly conserved among this class of homeoproteins. Interestingly, Ajuba has been reported to associate with thyroid transcription factor-1/Nkx2-1, a member of NK homeobox transcription factors, in mammalian cells, although the physiological function of their interaction remains unknown (Missero et al., 2001). It is possible that there are more combinatorial patterns of physical interaction between Zyxin family LIM proteins and NK homeoproteins.

Cal shuttles between the cytoplasm and the nucleus

The leucine-rich sequence of Cal is thought to function as an NES, based on the following results: (a) the leucine-rich sequence of Cal matches the consensus of the NES; (b) predominant nuclear distribution was observed when treated with LMB, that is a specific inhibitor of CRM1-dependent nuclear export (Kudo et al., 1998); (c) the Cal mutant lacking the leucine-rich sequence was localized predominantly in the nucleus; and (d) fusion of leucine-rich sequence of Cal to Rev1.4-EGFP transported the Rev1.4-EGFP from the nucleus to the cytoplasm (Henderson, 2000). Functional leucine-rich NESs have been identified in other Zyxin family members such as *Zyxin* (Nix and Beckerle, 1997), *trip6* (Wang and Gilmore, 2001), *LPP* (Petit et al., 2000), and *Ajuba* (Kanungo et al., 2000). Although the role of Zyxin family members in the nucleus has not been fully defined, the interaction between Zyxin and h-wartz/LATS1 on the mitotic apparatus implicates the specific role of Zyxin in the regulation of cell cycle (Hirota et al., 2000).

Cal augments CSX/NKX2-5–induced promoter activation

The interaction between CSX/NKX2-5 and Cal implicates a certain role of transcriptional regulation of cardiac-specific genes. CSX/NKX2-5 and Cal synergistically activated both the *ANP* promoter and the artificial promoter containing multimerized CSX/NKX2-5–binding sites. Furthermore, Cal enhanced cooperative promoter activation of *ANP* gene between CSX/NKX2-5 and GATA-4 or Tbx-5. These results suggest that transcriptional regulation by cardiac transcription factors may be fulfilled harmoniously by multiprotein complex.

The GAL4-based reporter assay revealed that Cal itself possesses transcriptional activity. LIM2 and LIM3 domains were endowed with the capacity to activate transcription, whereas the LIM1 domain suppressed the transcriptional activity. On the other hand, the ΔLIM1 mutant failed to augment CSX/NKX2-5–induced transactivation of the *ANP* reporter (Fig. 3 B). GST pull-down assays revealed that the LIM domains are required for binding to CSX/NKX2-5 and that deletion of LIM1 reduced the mutual binding (Fig. 2 C), suggesting that deletion of LIM1 may also decrease the binding affinity for CSX/NKX2-5. In addition, there is a possibility that the LIM1 interferes the GAL4-DNA binding but not inhibits the transcription. It has been reported that Trip6 and LPP have transcriptional activity, and the transactivation domains were attributed to the LIM domains and a region containing the NES of *trip6* (Wang and Gilmore, 2001) and to the LIM domains and the proline-rich region of *LPP* (Kanungo et al., 2000). Based on the fact that transactivation domains reside in modules for protein–protein interaction, it is likely that the interaction with components of transcriptional initiation complex is involved in transcriptional activation.

Cooperative transactivation of the *ANP* promoter by CSX/NKX2-5 and Cal was enhanced when Cal protein was targeted into the nucleus by deleting its NES. We found that treatment with Ca^{2+} ionophore A23187 induced nuclear transport of Cal. Pathophysiological significance of Ca^{2+} signaling in cardiac development has not been fully defined. However, Ca^{2+} signals are induced by various conditions including G-protein–coupled receptors (Clapham, 1995) and receptor tyrosine kinases (Schlessinger, 2000). It is possible to assume that Cal might modulate the transcriptional activity of CSX/NKX2-5 in response to Ca^{2+} signals triggered by G-protein–coupled receptors or receptor tyrosine kinases during cardiogenesis. Exploration of physiological ligands that activate Ca^{2+} signals and subsequent nuclear import of Cal will undermine the molecular framework of cardiac development.

Ca^{2+} signaling plays an important role in generation of cardiac hypertrophy (Frey et al., 2000). Nuclear import of NF-AT transcription factors is induced by Ca^{2+}-activated phosphatase calcineurin and that transgenic mice expressing nuclear form of NF-AT3 in the heart exhibited cardiac hypertrophy (Molkentin et al., 1998). CSX/NKX2-5 is expressed in the adult heart (Komuro and Izumo, 1993), and it has been proposed that CSX/NKX2-5 is involved in generation of cardiac hypertrophy (Akazawa and Komuro, 2003) on the basis of in vivo findings that expression levels of CSX/NKX2-5 were increased in response to hypertrophic stimuli including pressure overload (Thompson et al., 1998) and phenylephrine or isoproterenol (Saadane et al., 1999). Therefore, Cal may be another Ca^{2+}-sensitive effector that translocates into the nucleus like NF-AT transcription factors and it is possible to speculate that Cal may play a certain role in generation of cardiac hypertrophy by modulating transcriptional activity of CSX/NKX2-5.

Cal may function as a signal mediator that links cytoplasmic signals and gene expression

Cal was localized in the cytoplasm at steady state and translocated into the nucleus in response to calcium, and Cal functioned as a transcriptional activator in the nucleus by cooper-

ating with the cardiac transcription factor CSX/NKX2-5. These results indicate a novel function of LIM proteins that link cytoplasmic signals and nuclear gene expression.

Recently, some proteins associated with cell junctions have been reported to be involved in transcriptional regulation. A membrane-associated guanylate kinase, CASK/LIN-2, interacts with a T-box transcription factor, Tbr-1, and stimulates the transcriptional activity of Tbr-1 in the nucleus of mammalian cells (Hsueh et al., 2000). Jun activation domain-binding protein 1, colocalizing with integrin LFA-1, translocates into the nucleus in response to LFA-1 stimulation and acts as a coactivator for AP-1 complex (Bianchi et al., 2000). β-Catenin, linking cadherins to actin cytoskeleton at adherens junctions, interacts with T cell factor to form a transcriptional activator complex in response to Wnt signaling (Barth et al., 1997). Although CRP3/MLP binds to Zyxin and α actinin in the cytoplasm (Louis et al., 1997), forced expression of CRP3/MLP in the nucleus by fusing it to nuclear localization signal led to a cooperative enhancement of the transcriptional activity of MyoD (Kong et al., 1997). Trip6 also acts as a coactivator for v-Rel transcription factor (Zhao et al., 1999). However, it remains unclear how subcellular localization of CRP3/MLP and trip6 is regulated. We first clarify the molecular mechanism of how the cytoplasmic LIM protein is translocated into the nucleus and functions as a transcriptional activator.

Cal promotes cardiac differentiation in P19CL6 cells

Mouse P19CL6 cells, derived from P19 embryonal carcinoma cells, are used as a good in vitro system for molecular analysis of cardiac differentiation. In the presence of 1% DMSO, mouse P19CL6 cell efficiently differentiate into spontaneously beating cardiac myocytes that exhibit the biological features recapturing embryonic cardiogenesis in vivo (Monzen et al., 1999, 2001). P19CL6 cells that overexpress nuclear form of Cal (P19CL6-Cal-ΔNES) differentiated into cardiac myocytes more efficiently than the parental P19CL6 cells. In P19CL6-Cal-ΔNES cells, expression levels of *SERCA2*, *calreticulin*, *connexin43*, *ANP*, and *cardiac troponin T* were up-regulated, which convey properties characteristic of cardiomyocytes. Expression levels of cardiac transcription factor *MEF2C* did not change, whereas expression levels of *GATA-4* were increased. Although there has been no evidence indicating that *GATA-4* is a downstream target for CSX/NKX2-5, it is possible that expression of *GATA-4* is up-regulated through undefined functions of Cal. Up-regulation of *GATA-4* might have an influence on myocardial cell differentiation in P19CL6-Cal-ΔNES. These results leave an open question whether the nuclear target for Cal is solely CSX/NKX2-5. However, based on the up-regulated expression of the target genes for CSX/NKX2-5, it is reasonable to assume that cooperation of CSX/NKX2-5 and Cal promoted cardiac differentiation in P19CL6 cells. Our present studies elucidate a novel role of LIM proteins in cardiac development as a transcriptional activator, and suggest that fine-tuned gene expression during cardiogenesis is orchestrated by multiprotein complex including LIM proteins as well as transcription factors.

Materials and methods

Molecular cloning of Cal

We performed a yeast two-hybrid screening using the MATCHMAKER Two-Hybrid System (CLONTECH Laboratories, Inc.) as described previously (Hiroi et al., 2001). The plasmid pGBT9-CSX, which encodes the GAL4 DNA-binding domain fused to the human CSX/NKX2-5, was used as a bait in screening of a human heart MATCHMAKER cDNA Library (CLONTECH Laboratories, Inc.). One clone containing a fragment of CAL cDNA was scored positive, and the full-length mouse Cal cDNA was obtained by screening a mouse heart cDNA library (Stratagene).

Northern blot, RT-PCR, and in situ hybridization analysis

For Northern blot analysis, total RNA was hybridized with cDNA corresponding to 3′-UTR of *Cal*. Probes for *GATA-4*, *MEF2C*, *connexin 43*, and *SERCA2* were described previously (Hiroi et al., 2001). A probe for *calreticulin* was a gift from M. Michalak (University of Alberta, Alberta, Canada). RT-PCR analysis for *ANP* expression was performed as described previously (Hiroi et al., 2001). Digoxygenin labeled riboprobes were synthesized by using the 1.5-kb *Cal* cDNA, and RNA in situ hybridization was performed as described previously (Akazawa et al., 2000).

Plasmids construction

The following plasmids were described previously: the expression vectors of CSX/NKX2-5 (pEFSA-HA-CSX), GATA-4 (pSSRa-hGATA4), and Tbx-5 (pcDNA3-Tbx5); the luciferase reporters containing the *ANP* promoter (ANP[600]-Luc and ANP[2600]-Luc); and multimerized CSX-binding sites (4×TTF-Luc; Shiojima et al., 1999; Hiroi et al., 2001). FLAG-tagged Cal was subcloned into pCAGGS vector (pCAGGS-FLAG-Cal; Niwa et al., 1991; Aoki et al., 2000). pCAGGS vector was provided by J. Miyazaki (Osaka University Graduate School of Medicine, Suita, Japan) and T. Kobayashi and O. Hino (The Cancer Institute, Japanese Foundation for Cancer Research, Tokyo, Japan). Cal derivatives were subcloned into pcDNA3.1 (Invitrogen) and pBIND (Promega) for in vitro transcription and translation and expression of GAL4-fusion protein, respectively. For deletion analyses, the following Cal derivatives were subcloned into the corresponding vectors: Cal-ΔLIM1 (1-184, 221-375), Cal-ΔLIM2 (1-244, 279-375), Cal-ΔLIM3 (1-307, 345-375), Cal-ΔLIM123 (1-184), Cal-LIM123 (185-375), Cal-LIM23 (245-375), and Cal-ΔNES (1-121, 135-375).

Cell culture, transfection, and reporter gene assay

Primary cultures of cardiac myocytes were prepared from ventricles of 1-d-old Wistar rats as described previously (Kudoh et al., 1997). Transient transfections were performed by standard calcium phosphate methods. For reporter gene assays, pRL-SV40 (Promega) was cotransfected as an internal control. Luciferase activities were measured as described previously (Shiojima et al., 1999). P19CL6 cells were cultured as described previously (Monzen et al., 1999). To isolate the permanent cell lines, P19CL6 cells were transfected with pcDNA3.1-Cal and pcDNA3.1-Cal-ΔNES by the lipofection method (TfxTM reagents; Promega). Stable transformants were selected with 400 μg/ml of neomycin (G418; Sigma-Aldrich).

Coimmunoprecipitation experiment

We performed a coimmunoprecipitation experiment as described previously (Shiojima et al., 1999). COS-7 cells were transiently transfected with expression plasmids of pEFSA-HA-CSX and pCAGGS-FLAG-Cal or pCAGGS-FLAG-CalΔNES. For preparation of the cytoplasmic fraction, transfected cells were lysed in digitonin buffer (20 mM Hepes/KOH, pH 7.5, 150 mM NaCl, 1 mM EDTA, and 50 μg/ml digitonin) on ice for 10 min. The lysates were centrifuged at 1,000 *g* and the supernatant was collected as the cytoplasmic fraction. The pellets were resuspended Triton buffer (20 mM Hepes/KOH, pH 7.5, 150 mM NaCl, 1 mM EDTA, and 10 mg/ml Triton X-100) and the lysates were used as the nuclear fraction. Protein samples were subjected to immunoprecipitation with the anti-FLAG mAb M2 (KODAK), fractionated by 10% SDS-PAGE, and immunoblotted with the rabbit polyclonal anti-HA antibody (Santa Cruz Biotechnology, Inc.). HRP-conjugated anti-rabbit IgG antibody was used as the secondary antibody and immune complex was detected by the ECL detection kit (Amersham Biosciences).

GST pull-down assay

We performed GST pull-down assays as described previously (Shiojima et al., 1999). GST fusion protein of CSX/NKX2-5 has been described previously. cDNA fragment corresponding to the full length of Cal was subcloned in frame into the EcoRI site of pGEX-3X (Amersham Biosciences). CSX/NKX2-5 derivatives (Shiojima et al., 1999) and Cal derivatives, subcloned

into pcDNA3.1 vector (Invitrogen), were labeled with [^{35}S]methionine by the TNT Quick Coupled Transcription/Translation Systems (Promega). GST and GST fusion proteins immobilized on glutathione-Sepharose 4B beads were mixed with in vitro–translated proteins. Bound proteins were fractionated by SDS-PAGE and visualized by autoradiography.

Immunostaining

Rat neonatal cardiac myocytes or HeLa cells were transfected with the expression vector of Cal and Cal mutants. Cells were stained with the anti-FLAG mAb M2 (KODAK), and visualized with FITC-labeled anti–mouse IgG (CAPPEL). Calcium ionophore A23187 was purchased from Sigma-Aldrich. Differentiated P19CL6 cells were stained with anticardiac troponin T mAb (Deutsche Sammlung von Mikroorganismen und Zellkulturen GmbH) and visualized with Cy3-labeled anti–mouse IgG (CHEMICON International, Inc.). The cells were double stained using rhodamine-phalloidin (Molecular Probes) or TO-PRO-3 (Molecular Probes).

Nuclear export assays

Nuclear export assays were performed as described previously (Henderson, 2000). pRev(1.4)-NES-EGFP plasmid was constructed by subcloning the NES of Cal between BamHI and AgeI sites of pRev(1.4)-EGFP plasmid (provided by B.R. Henderson, Westmead Institute for Cancer Research, Sydney, Australia). The NES of Cal was amplified by PCR using specific primers (5′-AGGGAAGCCCCCACCCCCGCCTC-3′, and 5′-GGTGGGGGCTTCCCTG-GTAAGACA-3′). Actinomycin D (Sigma-Aldrich) was added at 5 mg/ml to prevent nucleolar association of Rev protein. LMB was provided by M. Yoshida (The University of Tokyo, Tokyo, Japan).

Acquisition and processing of images

For light microscopic analysis (Fig. 1 C), images were acquired by a stereomicroscope (MZ12; objective lens, Plan 1.0×; Leica) and captured by DC100 program (Leica), or by a light microscope (Axioskop 2 plus; objective lens, Plan-Neofluar 2.5×/0.075; Carl Zeiss MicroImaging, Inc.) and captured by Axio Cam CCD camera and Axio Vision 3.0 imaging system (Carl Zeiss MicroImaging, Inc.). For immunofluorescence microscopic analysis, images were acquired by a laser-scanning microscope (model Eclipse E600; Nikon) using Plan-Fluor 10×/0.30 (Fig. 7 B), Plan-Fluor 40×/0.75 (Fig. 6 A), and Plan-Apo 60×A/1.40 oil (Fig. 5). Radiance 2000 confocal scanning system (Bio-Rad Laboratories) was used.

Accession no.

The deduced amino acid sequence of mouse Cal was deposited in GenBank/EMBL/DDBJ accession no. AF513359.

We thank Ms. R. Kobayashi, E. Fujita, and M. Watanabe for their excellent technical assistance.

This work was supported in part by grants from the Japanese Ministry of Education, Science, Sports, and Culture, and Japan Health Sciences Foundation (JHSF; to I. Komuro), Japanese Heart Foundation and Kanae Foundation for Life and Sociomedical Science (to H. Akazawa). H. Akazawa is a Research Resident for Research on Human Genome, Tissue Engineering Food Biotechnology of JHSF.

Submitted: 26 September 2003
Accepted: 29 December 2003

References

Akazawa, H., and I. Komuro. 2003. Roles of cardiac transcription factors in cardiac hypertrophy. *Circ. Res.* 92:1079–1088.

Akazawa, H., I. Komuro, Y. Sugitani, Y. Yazaki, R. Nagai, and T. Noda. 2000. Targeted disruption of the homeobox transcription factor Bapx1 results in lethal skeletal dysplasia with asplenia and gastroduodenal malformation. *Genes Cells.* 5:499–513.

Aoki, H., J. Hayashi, M. Moriyama, Y. Arakawa, and O. Hino. 2000. Hepatitis C virus core protein interacts with 14-3-3 protein and activates the kinase Raf-1. *J. Virol.* 74:1736–1741.

Arber, S., and P. Caroni. 1996. Specificity of single LIM motifs in targeting and LIM/LIM interactions in situ. *Genes Dev.* 10:289–300.

Arber, S., G. Halder, and P. Caroni. 1994. Muscle LIM protein, a novel essential regulator of myogenesis, promotes myogenic differentiation. *Cell.* 79: 221–231.

Arber, S., J.J. Hunter, J. Ross, Jr., M. Hongo, G. Sansig, J. Borg, J.C. Perriard, K.R. Chien, and P. Caroni. 1997. MLP-deficient mice exhibit a disruption of cardiac cytoarchitectural organization, dilated cardiomyopathy, and heart failure. *Cell.* 88:393–403.

Bach, I. 2000. The LIM domain: regulation by association. *Mech. Dev.* 91:5–17.

Barth, A.I., I.S. Nathke, and W.J. Nelson. 1997. Cadherins, catenins and APC protein: interplay between cytoskeletal complexes and signaling pathways. *Curr. Opin. Cell Biol.* 9:683–690.

Beckerle, M.C. 1997. Zyxin: zinc fingers at sites of cell adhesion. *Bioessays.* 19: 949–957.

Bianchi, E., S. Denti, A. Granata, G. Bossi, J. Geginat, A. Villa, L. Rogge, and R. Pardi. 2000. Integrin LFA-1 interacts with the transcriptional co-activator JAB1 to modulate AP-1 activity. *Nature.* 404:617–621.

Bruneau, B.G., G. Nemer, J.P. Schmitt, F. Charron, L. Robitaille, S. Caron, D.A. Conner, M. Gessler, M. Nemer, C.E. Seidman, and J.G. Seidman. 2001. A murine model of Holt-Oram syndrome defines roles of the T-box transcription factor Tbx5 in cardiogenesis and disease. *Cell.* 106:709–721.

Chen, C.Y., and R.J. Schwartz. 1996. Recruitment of the tinman homolog Nkx-2.5 by serum response factor activates cardiac alpha-actin gene transcription. *Mol. Cell. Biol.* 16:6372–6384.

Clapham, D.E. 1995. Calcium signaling. *Cell.* 80:259–268.

Dawid, I.B., J.J. Breen, and R. Toyama. 1998. LIM domains: multiple roles as adapters and functional modifiers in protein interactions. *Trends Genet.* 14: 156–162.

Durocher, D., F. Charron, R. Warren, R.J. Schwartz, and M. Nemer. 1997. The cardiac transcription factors Nkx2-5 and GATA-4 are mutual cofactors. *EMBO J.* 16:5687–5696.

Fornerod, M., M. Ohno, M. Yoshida, and I.W. Mattaj. 1997. CRM1 is an export receptor for leucine-rich nuclear export signals. *Cell.* 90:1051–1060.

Frey, N., T.A. McKinsey, and E.N. Olson. 2000. Decoding calcium signals involved in cardiac growth and function. *Nat. Med.* 6:1221–1227.

Gertler, F.B., K. Niebuhr, M. Reinhard, J. Wehland, and P. Soriano. 1996. Mena, a relative of VASP and *Drosophila* Enabled, is implicated in the control of microfilament dynamics. *Cell.* 87:227–239.

Goyal, R.K., P. Lin, J. Kanungo, A.S. Payne, A.J. Muslin, and G.D. Longmore. 1999. Ajuba, a novel LIM protein, interacts with Grb2, augments mitogen-activated protein kinase activity in fibroblasts, and promotes meiotic maturation of *Xenopus* oocytes in a Grb2- and Ras-dependent manner. *Mol. Cell. Biol.* 19:4379–4389.

Henderson, B.R. 2000. Nuclear-cytoplasmic shuttling of APC regulates beta-catenin subcellular localization and turnover. *Nat. Cell Biol.* 2:653–660.

Hiroi, Y., S. Kudoh, K. Monzen, Y. Ikeda, Y. Yazaki, R. Nagai, and I. Komuro. 2001. Tbx5 associates with Nkx2-5 and synergistically promotes cardiomyocyte differentiation. *Nat. Genet.* 28:276–280.

Hirota, T., T. Morisaki, Y. Nishiyama, T. Marumoto, K. Tada, T. Hara, N. Masuko, M. Inagaki, K. Hatakeyama, and H. Saya. 2000. Zyxin, a regulator of actin filament assembly, targets the mitotic apparatus by interacting with h-warts/LATS1 tumor suppressor. *J. Cell Biol.* 149:1073–1086.

Hobert, O., J.W. Schilling, M.C. Beckerle, A. Ullrich, and B. Jallal. 1996. SH3 domain-dependent interaction of the proto-oncogene product Vav with the focal contact protein zyxin. *Oncogene.* 12:1577–1581.

Hsueh, Y.P., T.F. Wang, F.C. Yang, and M. Sheng. 2000. Nuclear translocation and transcription regulation by the membrane-associated guanylate kinase CASK/LIN-2. *Nature.* 404:298–302.

Kanungo, J., S.J. Pratt, H. Marie, and G.D. Longmore. 2000. Ajuba, a cytosolic LIM protein, shuttles into the nucleus and affects embryonal cell proliferation and fate decisions. *Mol. Biol. Cell.* 11:3299–3313.

Komuro, I., and S. Izumo. 1993. Csx: a murine homeobox-containing gene specifically expressed in the developing heart. *Proc. Natl. Acad. Sci. USA.* 90: 8145–8149.

Kong, Y., M.J. Flick, A.J. Kudla, and S.F. Konieczny. 1997. Muscle LIM protein promotes myogenesis by enhancing the activity of MyoD. *Mol. Cell. Biol.* 17:4750–4760.

Kudo, N., B. Wolff, T. Sekimoto, E.P. Schreiner, Y. Yoneda, M. Yanagida, S. Horinouchi, and M. Yoshida. 1998. Leptomycin B inhibition of signal-mediated nuclear export by direct binding to CRM1. *Exp. Cell Res.* 242:540–547.

Kudoh, S., I. Komuro, T. Mizuno, T. Yamazaki, Y. Zou, I. Shiojima, N. Takekoshi, and Y. Yazaki. 1997. Angiotensin II stimulates c-Jun NH2-terminal kinase in cultured cardiac myocytes of neonatal rats. *Circ. Res.* 80:139–146.

Kuersten, S., M. Ohno, and I.W. Mattaj. 2001. Nucleocytoplasmic transport: Ran, beta and beyond. *Trends Cell Biol.* 11:497–503.

Lee, Y., T. Shioi, H. Kasahara, S.M. Jobe, R.J. Wiese, B.E. Markham, and S. Izumo. 1998. The cardiac tissue-restricted homeobox protein Csx/Nkx2.5 physically associates with the zinc finger protein GATA4 and cooperatively activates atrial natriuretic factor gene expression. *Mol. Cell. Biol.* 18:3120–3129.

Lints, T.J., L.M. Parsons, L. Hartley, I. Lyons, and R.P. Harvey. 1993. Nkx-2.5: a novel murine homeobox gene expressed in early heart progenitor cells and their myogenic descendants. *Development.* 119:969.

Louis, H.A., J.D. Pino, K.L. Schmeichel, P. Pomies, and M.C. Beckerle. 1997. Comparison of three members of the cysteine-rich protein family reveals functional conservation and divergent patterns of gene expression. *J. Biol. Chem.* 272:27484–27491.

Lyons, I., L.M. Parsons, L. Hartley, R. Li, J.E. Andrews, L. Robb, and R.P. Harvey. 1995. Myogenic and morphogenetic defects in the heart tubes of murine embryos lacking the homeo box gene Nkx2-5. *Genes Dev.* 9:1654–1666.

Mahoney, N.M., P.A. Janmey, and S.C. Almo. 1997. Structure of the profilin-poly-L-proline complex involved in morphogenesis and cytoskeletal regulation. *Nat. Struct. Biol.* 4:953–960.

Mattaj, I.W., and L. Englmeier. 1998. Nucleocytoplasmic transport: the soluble phase. *Annu. Rev. Biochem.* 67:265–306.

Missero, C., M.T. Pirro, S. Simeone, M. Pischetola, and R. Di Lauro. 2001. The DNA glycosylase T:G mismatch-specific thymine DNA glycosylase represses thyroid transcription factor-1-activated transcription. *J. Biol. Chem.* 276: 33569–33575.

Molkentin, J.D., J.R. Lu, C.L. Antos, B. Markham, J. Richardson, J. Robbins, S.R. Grant, and E.N. Olson. 1998. A calcineurin-dependent transcriptional pathway for cardiac hypertrophy. *Cell.* 93:215–228.

Monzen, K., I. Shiojima, Y. Hiroi, S. Kudoh, T. Oka, E. Takimoto, D. Hayashi, T. Hosoda, A. Habara-Ohkubo, T. Nakaoka, et al. 1999. Bone morphogenetic proteins induce cardiomyocyte differentiation through the mitogen-activated protein kinase kinase kinase TAK1 and cardiac transcription factors Csx/Nkx-2.5 and GATA-4. *Mol. Cell. Biol.* 19:7096–7105.

Monzen, K., Y. Hiroi, S. Kudoh, H. Akazawa, T. Oka, E. Takimoto, D. Hayashi, T. Hosoda, M. Kawabata, K. Miyazono, et al. 2001. Smads, TAK1, and their common target ATF-2 play a critical role in cardiomyocyte differentiation. *J. Cell Biol.* 153:687–698.

Niwa, H., K. Yamamura, and J. Miyazaki. 1991. Efficient selection for high-expression transfectants with a novel eukaryotic vector. *Gene.* 108:193–199.

Nix, D.A., and M.C. Beckerle. 1997. Nuclear-cytoplasmic shuttling of the focal contact protein, zyxin: a potential mechanism for communication between sites of cell adhesion and the nucleus. *J. Cell Biol.* 138:1139–1147.

Ohno, M., M. Fornerod, and I.W. Mattaj. 1998. Nucleocytoplasmic transport: the last 200 nanometers. *Cell.* 92:327–336.

Petit, M.M., R. Mols, E.F. Schoenmakers, N. Mandahl, and W.J. Van de Ven. 1996. LPP, the preferred fusion partner gene of HMGIC in lipomas, is a novel member of the LIM protein gene family. *Genomics.* 36:118–129.

Petit, M.M., J. Fradelizi, R.M. Golsteyn, T.A. Ayoubi, B. Menichi, D. Louvard, W.J. Van de Ven, and E. Friederich. 2000. LPP, an actin cytoskeleton protein related to zyxin, harbors a nuclear export signal and transcriptional activation capacity. *Mol. Biol. Cell.* 11:117–129.

Prehoda, K.E., D.J. Lee, and W.A. Lim. 1999. Structure of the enabled/VASP homology 1 domain-peptide complex: a key component in the spatial control of actin assembly. *Cell.* 97:471–480.

Renfranz, P.J., and M.C. Beckerle. 2002. Doing (F/L)PPPPs: EVH1 domains and their proline-rich partners in cell polarity and migration. *Curr. Opin. Cell Biol.* 14:88–103.

Saadane, N., L. Alpert, and L.E. Chalifour. 1999. Expression of immediate early genes, GATA-4, and Nkx-2.5 in adrenergic-induced cardiac hypertrophy and during regression in adult mice. *Br. J. Pharmacol.* 127:1165–1176.

Sadler, I., A.W. Crawford, J.W. Michelsen, and M.C. Beckerle. 1992. Zyxin and cCRP: two interactive LIM domain proteins associated with the cytoskeleton. *J. Cell Biol.* 119:1573–1587.

Schlessinger, J. 2000. Cell signaling by receptor tyrosine kinases. *Cell.* 103:211–225.

Schott, J.J., D.W. Benson, C.T. Basson, W. Pease, G.M. Silberbach, J.P. Moak, B.J. Maron, C.E. Seidman, and J.G. Seidman. 1998. Congenital heart disease caused by mutations in the transcription factor NKX2-5. *Science.* 281: 108–111.

Shiojima, I., I. Komuro, T. Oka, Y. Hiroi, T. Mizuno, E. Takimoto, K. Monzen, R. Aikawa, H. Akazawa, T. Yamazaki, et al. 1999. Context-dependent transcriptional cooperation mediated by cardiac transcription factors Csx/Nkx-2.5 and GATA-4. *J. Biol. Chem.* 274:8231–8239.

Thompson, J.T., M.S. Rackley, and T.X. O'Brien. 1998. Upregulation of the cardiac homeobox gene Nkx2-5 (CSX) in feline right ventricular pressure overload. *Am. J. Physiol.* 274:H1569–H1573.

Wang, Y., and T.D. Gilmore. 2001. LIM domain protein Trip6 has a conserved nuclear export signal, nuclear targeting sequences, and multiple transactivation domains. *Biochim. Biophys. Acta.* 1538:260–272.

Yi, J., and M.C. Beckerle. 1998. The human TRIP6 gene encodes a LIM domain protein and maps to chromosome 7q22, a region associated with tumorigenesis. *Genomics.* 49:314–316.

Zhao, M.K., Y. Wang, K. Murphy, J. Yi, M.C. Beckerle, and T.D. Gilmore. 1999. LIM domain-containing protein trip6 can act as a coactivator for the v-Rel transcription factor. *Gene Expr.* 8:207–217.